Elsevier Editorial System(tm) for Stem Cell Research
Manuscript Draft

Manuscript Number:

Title: Comprehensive transcriptome and immunophenotype analysis of renal and cardiac MSC-like populations supports strong congruence with bone marrow MSC despite maintenance of distinct identities

Article Type: Regular Article

Corresponding Author: Dr. Melissa H Little, PhD

Corresponding Author's Institution: The University of Queensland

First Author: Rebecca Pelekanos, PhD

Order of Authors: Rebecca Pelekanos, PhD; Joan Li, PhD; Milena Gongora, PhD; Vashe Chandrakanthan, PhD; Janelle Scown, BSc; Norseha Suhaimi, BSc; Gary Brooke, PhD; Melinda E Christensen, BSc; Tram Doan, PhD; Alison M Rice, PhD; Geoffrey W Osborne, PhD; Sean M Grimmond, PhD; Richard P Harvey, PhD; Kerry Atkinson, MBBS; Melissa H Little, PhD

Abstract: Cells resembling bone marrow mesenchymal stem cells (MSC) have been isolated from many organs but their functional relationships have not been thoroughly examined. Here we compared the immunophenotype, gene expression, multipotency and immunosuppressive potential of MSC-like colony-forming cells from adult murine bone marrow (bmMSC), kidney (kCFU-F) and heart (cCFU-F), cultured under uniform conditions. All populations showed classic MSC morphology and in vitro mesodermal multipotency. Of the two solid organ-specific CFU-F, only kCFU-F displayed suppression of T-cell alloreactivity in vitro, albeit to a lesser extent than bmMSC. Quantitative immunophenotyping using 81 phycoerythrin-conjugated CD antibodies demonstrated that all populations contained high percentages of cells expressing diagnostic MSC surface markers (Sca1, CD90.2, CD29, CD44), as well as others noted previously on murine MSC (CD24, CD49e, CD51, CD80, CD81, CD105). Illumina microarray expression profiling and bioinformatic analysis indicated a correlation of gene expression of 0.88-0.92 between pairwise comparisons. All populations expressed approximately 66% of genes in the pluripotency network (Plurinet), presumably reflecting their stem-like character. Furthermore, all populations expressed genes involved in immunomodulation, homing and tissue repair, suggesting these as conserved functions for MSC-like cells in solid organs. Despite this molecular congruence, strong biases in gene and protein expression and pathway activity were seen, suggesting organ-specific functions. Hence, tissue-derived MSC may also retain unique properties potentially rendering them more appropriate as cellular therapeutic agents for their organ of origin.

Suggested Reviewers: Andrew Elefanty
Andrew.Elefanty@med.monash.edu.au
Submission was at the request of the Editor in Chief

Stan Gronthos
stan.gronthos@health.sa.gov.au
System requires two other reviewers. Stan is an expert in MSC biology

Simon Cool
scool@imcb.a-star.edu.sg

Works in stem cell differentiation, especially to cartilage and bone

Professor Andrew Elefanty
Editor in Chief, Stem Cell Research

29 July 2011

Dear Andrew,

Re: Pelekanos et al, Comprehensive transcriptome and immunophenotype analysis of renal and cardiac MSC-like populations supports strong congruence with bone marrow MSC despite maintenance of distinct identities.

On behalf of the authors, I thank you for accepting this manuscript as a new submission. Based upon your editorial review of the previous version, we believe that we have been able to address your remaining concerns either via modifications to the manuscript or via the direct responses listed below. This has included the modification of Figure 1 to clarify the experimental plan and the addition of a further Supplementary Figure to compare the results obtained using the initial immunophenotyping and the immunophenotypic screen. Detailed responses to each of the issues that you raised are in the accompanying document.

I do feel confident that this manuscript will represent an important resource for your readership and I trust you will agree. I would note that, as indicated in the text, all of the microarray data has been submitted to GEO as a public resource. We look forward to hearing from you,

Kind regards,

Melissa Little

Professor Melissa Helen Little
Principal Research Fellow
Institute for Molecular Bioscience
The University of Queensland
St. Lucia, Qld. 4072
Australia
Ph: +617 3346 2054
FAX: +617 3346 2101
Mobile: 0427770386

With respect to the specific issues you raised in your email of 25 July, detailed below are our responses. All changes made to the text of the manuscript or Supplementary Data have been highlighted in red.

Comment: Generation of cultures from the three tissues. I suggest the inclusion as a new Figure 1 of a scheme (perhaps shown as a timeline) depicting the derivation of the three MSC populations, based on the detailed methods provided in Supp Data. For example, from my reading, this indicates that the bmMSC were sorted CD45-Sca1+ from the adherent culture, the cardiac cells were CD45-CD31-PDGFRa+Sca1+ and the kidney cells were CD45-CD31-CD24loSca1+. You could include in this figure the subsequent time points for immunophenotypic and microarray analyses. The inclusion of this figure would make it clear to the reader what was being compared and would make the whole manuscript easier to follow.

Response: We have modified Figure 1 to provide such a flow chart (now Figure 1A).

Comment: Please also clarify in the text (perhaps in the methods also) approximately how many CFU-F would have been pooled to generate MSC populations from the three tissues and how many independently initiated cultures would have been used to generate the various data sets. The point of this question is to provide the reader an indication of the likely generality of the findings.

Response: Additional text has now been added to the Methods section indicating the material collected from each tissue type to represent a single biological replicate. We would note that all the data presented is averaged from biological replicates with each biological replicate representing an independently initiated culture. In the case of microarray, data presented is from triplicates; in the case of the immunophenotyping, duplicate samples.

Comment: You state that PDGFRa was used to isolate the cardiac CFU-F containing population, therefore it is surprising that the immunophenotypic analysis of these cells revealed them to be essentially PDGFRa negative, especially since MSC from the other populations contained 30-40% PDGFRa+ cells (Supp Table 2). Please comment on this.

Response: We do not believe that the CD140a results seen for the cCFU-F, or the other two cell types, is inaccurate. While the cCFU-F were initially isolated based upon the expression of PDGFRα (PDGFRα-GFP), the nature of MSC cultures is that the long term repopulating stem cells will represent only a subset of the culture. For immunophenotyping, cells were passaged with TrypLE Select (Invitrogen) to avoid epitope cleavage. Confirming the reduction in the percentage of PDGFRa+ cells over time is a decline in the level of GFP positivity with passage, and based upon FITC analysis, the replicate passages used for immunophenotyping were only 23.7% GFP positive. We do now comment upon this in the Results section of the manuscript (p7).

Comment: In this same Supp Table 2, the epitope density for the PDGFRa+ cells on bmMSC is indicated at 1.0 - this seems to be incorrect, since the positive cells must be brighter than the negative cells in the population or the unstained controls. Please clarify/correct this.

Response: The value of 1.0 in the tabulated data occurs as a consequence of the gating strategy employed to generate the statistics. Based on control cell intrinsic fluorescence intensity distributions, a stringent analysis region (boxed) was drawn on the premise that fluorescent signals detected within this region represent antibody binding. Mean fluorescence intensity was calculated for the population residing in this region. Upon antibody binding, varying mean values are reported for the cells falling within the region, and are occasionally skewed to a value of one when the intensity is low and a very small population of control cells also are detected within the region. This is illustrated in the provided figure which represents the data point in question (bmMSC CD140a). The top panels show replicate non-stained controls, while the lower panels show clear antibody binding of the population as a whole. Yet due to the mean intensity of the minor population in the control panel, we report a conservative statistic for the relative mean fluorescence intensity of the test cells binding the antibody. On this occasion, this results in a value of 1.

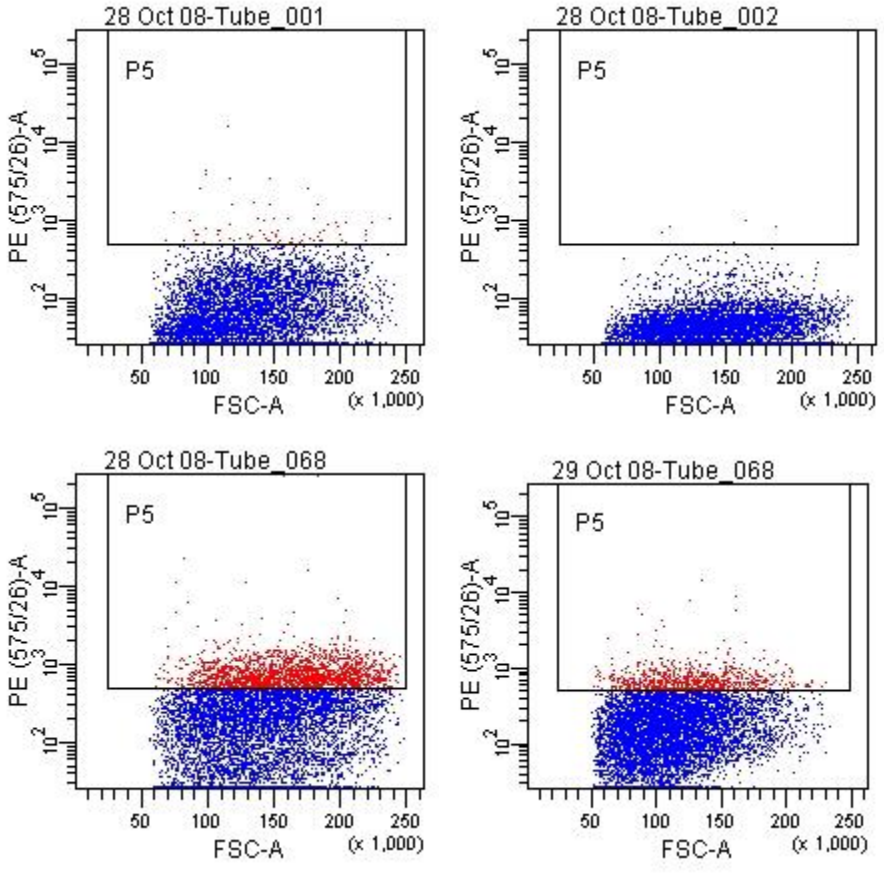

Comment: An area of concern raised by the reviewer that needs resolution related to the methods of immunophenotypic analysis. From my reading, in the initial immunophenotyping analysis you used 7AAD to exclude dead cells and isotype controls to assist in setting gates. It is

not clear why you changed your method of analysis for the panel arrays to include a paraformaldehyde fixation step (precluding you from using dye exclusion for live cell analysis) and used an unstained control rather than isotypes as a negative. You may wish to comment on this.

Response: The inclusion of a paraformaldehyde fixation step was deemed necessary during such an extensive plate screening platform after the realization that significant periods of time were involved where stained samples sit on the instrument prior to analysis. In this format there is no temperature control and as such receptor shedding and antibody capping on unfixed cells from varying sources were areas of concern that we sought to minimize by staining then fixing the cells prior to analysis.

While isotype controls can be beneficial in discovering problems associated with antibody staining they are not appropriate in the screening scenario for the following reasons. The point of using an isotype control is to determine the amount of background binding that occurs when a cell is exposed to an antibody of a particular specificity, and is reported by a fluorochrome conjugated to the isotype control antibody. The panel design relies on screening cells from varied sources with antibodies of various isotypes and manufacturers, directly conjugated to phycoerythrin (PE). PE-conjugated antibodies are in the majority of cases conjugates of a single PE molecule to a single antibody which eliminates the problem of various fluorochrome to protein ratios (F/P) seen with other combinations. However even with the same F/P conjugates, one may have the PE conjugated at a critical "background" binding site, while another does not, and this can dramatically affect the "stickiness" and amount of background one sees. Coupled with this, we have the problem of variation in intrinsic fluorescence that the different cell populations possess, due in part to NADPH levels and flavin content, which can vary the background considerably. With these factors in mind we then consider any antibodies within the panel that did not exhibit binding as de facto "isotype" controls.

In addition, we considered the problem of what would be an appropriate concentration to use for any selected isotype control. For the regular antibodies we choose the "saturating" concentration, however for the isotype control antibody there is no such thing as saturation; the more antibody you use, the more background you get. If we had used an isotype control we could have matched the concentration to that of the test antibody, on the false assumption that the proper minimal saturating concentration for one would mimic another. Do you therefore prepare a different isotype stain for each different concentration of conjugated antibody and across varying manufacturers? We did not, and posit that the isotype control is not a valid or applicable "control" in our screening panel.

Comment: Nevertheless, the only practical implication in my opinion is that you demonstrate that you could similarly detect surface molecules using both methods. For example, you state that Supp Figure 1 shows histograms from the initial immunophenotyping. (Incidentally, in Supp data you indicate that this included PE and APC conj antibodies, but Fig legend to supp fig

1states all were PE conj. Please clarify this.). Therefore, please provide some of the histograms from the panel analyses to show that there was a similar ability to detect the same positive and negative surface markers as are shown for the initial immunophenotyping. This could be included as a Supp Figure.

Response: In order to directly address the question of whether there is equivalence between the initial immunophenotyping and the immunophenotypic screen, a Supplementary Figure (S5) has been compiled directly comparing the results from the two methods for all epitopes investigated in the initial immunophenotyping. This comparison does show that both approaches detected the same epitopes on all cell populations.

We have corrected the Figure legend for Supplementary Figure 1 pertaining to APC versus PE-conjugated antibodies.

Comment: I note that in you methods you indicate that 40 cycles of amplification were used in your PCR analysis. This is generally considered excessive, especially given that the amount of starting material would not have been limiting. To me it implies that some of the very low intensity signals could arguably be considered absent. Please comment on this.

Response: The Supplementary qPCR data presented in Supplementary Figures S2-4 was performed with several objectives in mind. Supplementary Figure S2 is primarily to demonstrate that there is concordance between the microarray results and qPCR for low, medium and high expressors and that any differences in expression levels between the three cell types for a given gene are also accurately replicated using qPCR. Supplementary Figure S3 aims to validate the expression of a set of previously defined markers of MSCs and/or pericytes. In contrast, Supplementary Figure S4 aims to validate the expression of Plurinet genes, and to investigate the expression of the four Yamanaka genes, two of which were considered as not expressed based upon microarray data. We agree that for most genes, 30 cycles would have been sufficient. However, as the validation was being applied to genes detected as having low/no expression by microarray, 40 cycles was used in all instances. The text has been modified to make that point more forcefully (p10) and Supplementary Figure S4 has been annotated to indicate those genes for which microarray data indicated an Illumina detection score <0.

Comprehensive transcriptome and immunophenotype analysis of renal and cardiac MSC-like populations supports strong congruence with bone marrow MSC despite maintenance of distinct identities

Rebecca A. Pelekanos[b,c,i*], Joan Li[a,b*], Milena Gongora[a,b], Vashe Chandrakanthan[b,d], Janelle Scown[b,e], Norseha Suhaimi[ab], Gary Brooke[c], Melinda E. Christensen[f], Tram Doan[d], Alison M. Rice[f], Geoffrey W. Osborne[b,e], Sean M. Grimmond[a,b], Richard P. Harvey[b,d,g^], Kerry Atkinson[b,c,h^] and Melissa H. Little[a,b^#].

#corresponding author

[*]joint first authors representing equal contribution

^joint senior authors

[a] Institute for Molecular Bioscience, The University of Queensland, St Lucia, Brisbane, Queensland, Australia;

[b] Australian Stem Cell Centre, Monash University, Clayton, Victoria, Australia;

[c] Adult Stem Cell Laboratory, Mater Medical Research Institute, Brisbane, Queensland, Australia;

[d] Victor Chang Cardiac Research Institute, Sydney, New South Wales, Australia;

[e] Queensland Brain Institute, The University of Queensland, St Lucia, Brisbane, Queensland, Australia;

[f] Bone Marrow Transplantation Team, Mater Medical Research Institute, Brisbane, Queensland, Australia;

[g] Faculty of Medicine, University of New South Wales, Kensington, New South Wales, Australia;

[h] School of Medicine and Australian Institute of Nanotechnology and Bioengineering, The University of Queensland, St Lucia, Brisbane, Queensland, Australia;

[i] Current address: University of Queensland Centre for Clinical Research, The University of Queensland, Herston, Brisbane, Queensland, Australia.

Corresponding author:

Professor Melissa H Little

NHMRC Principal Research Fellow

Institute for Molecular Bioscience

The University of Queensland

St. Lucia, 4072

Australia

Ph: +61 7 3346 2054

FAX: +61 7 3346 2101

email: M.Little@imb.uq.edu.au

Running title: Comparisons between MSC-like populations

Key words: mesenchymal stem cell (MSC); colony forming unit-fibroblastic (CFU-F); kidney stem cell; cardiac stem cell; differentiation; immunophenotype; gene expression

Abstract

Cells resembling bone marrow mesenchymal stem cells (MSC) have been isolated from many organs but their functional relationships have not been thoroughly examined. Here we compared the immunophenotype, gene expression, multipotency and immunosuppressive potential of MSC-like colony-forming cells from adult murine bone marrow (bmMSC), kidney (kCFU-F) and heart (cCFU-F), cultured under uniform conditions. All populations showed classic MSC morphology and *in vitro* mesodermal multipotency. Of the two solid organ-specific CFU-F, only kCFU-F displayed suppression of T-cell alloreactivity *in vitro*, albeit to a lesser extent than bmMSC. Quantitative immunophenotyping using 81 phycoerythrin-conjugated CD antibodies demonstrated that all populations contained high percentages of cells expressing diagnostic MSC surface markers (Sca1, CD90.2, CD29, CD44), as well as others noted previously on murine MSC (CD24, CD49e, CD51, CD80, CD81, CD105). Illumina microarray expression profiling and bioinformatic analysis indicated a correlation of gene expression of 0.88-0.92 between pairwise comparisons. All populations expressed approximately 66% of genes in the pluripotency network (Plurinet), presumably reflecting their stem-like character. Furthermore, all populations expressed genes involved in immunomodulation, homing and tissue repair, suggesting these as conserved functions for MSC-like cells in solid organs. Despite this molecular congruence, strong biases in gene and protein expression and pathway activity were seen, suggesting organ-specific functions. Hence, tissue-derived MSC may also retain unique properties potentially rendering them more appropriate as cellular therapeutic agents for their organ of origin.

Introduction

Mesenchymal stem cells or multipotent mesenchymal stromal cells (both referred to as MSC) [1] are stem-like cells, traditionally of bone marrow origin, able to differentiate into a variety of mesenchymal lineages, including bone, fat and cartilage [2]. Originally designated Colony Forming Unit-Fibroblast (CFU-F) cells based upon their phenotype in culture [3, 4], attempts to identify, localize and purify MSC have been hampered by a lack of unique cell surface marker/s. Currently, the minimal criteria for human MSC are i) adherence to plastic with fibroblast-like morphology; ii) expression of CD105, CD73, CD90 and lack of expression of CD45, CD34, CD14 or CD11b, CD79a / CD19, HLA-DR; and iii) ability to differentiate into osteoblasts, adipocytes and chondrocytes *in vitro* [5, 6]. In the mouse, MSC are $Sca1^{+}CD90^{+}CD45^{-}$ [7]. While first described in the stroma of bone marrow, CFU-F have now been reported to exist in many fetal and adult tissues, including fat, bone, kidney, lung, liver, umbilical cord, amniotic fluid and placenta [8-12]. As proposed for bone marrow-derived MSC (bmMSC), such cells may act as tissue stem cells, provide a niche for other stem cells, or play a role in tissue homeostasis and repair. Recently, Crisan *et al* [13] prospectively isolated perivascular cells from a variety of human organs, including kidney, based on the expression of pericyte markers CD146, NG2 and PDGFRβ (CD140b), and showed that these cells displayed MSC features. Other studies also support the concept that MSCs arise from a perivascular niche [14].

Despite similarities between bmMSC and MSC-like populations from other locations, absolute phenotypic and functional equivalence has not been established. Indeed, evidence exists that there is a differentiative and reparative bias that depends upon the tissue of origin. Both fetal and bmMSC can induce repair after acute necrotizing injury of the heart, but via different mechanisms [15]. Placental and fetal MSC from amniotic fluid express pluripotency

genes (*Nanog*, SSEA-4 and *Oct4*), proliferate faster and show greater colony forming efficiency and osteogenic capacity [16, 17]. This suggests a more primitive stem-like phenotype and potentially enhanced utility in bone engineering applications [18, 19]. Placental MSC also show superior migratory capacity but less adipogenic potential [20-22]. Adipose MSC show greater capacity to form fat [23], while umbilical cord MSC show no such capacity [24]. Comparisons of gene expression between adipose, umbilical cord and bmMSC versus mature fibroblasts defined 25 genes uniformly present in these MSC [25, 26], but considerable differences in MSC phenotype and functional capacity were noted depending upon their tissue of origin [23, 25]. A microarray comparison between amniotic fluid, amniotic membrane and cord blood derived-MSC also suggested specific biological functions for MSC from different gestational tissues [27].

In this study we compare, both at the transcript and protein levels, distinct murine organ-specific MSC-like populations isolated from adult tissues (bone/bone marrow, heart and kidney). Although initial isolation approaches varied, once established as plastic adherent cultures displaying the anticipated cell surface antigens to define them as MSCs ($Sca1^{+}CD29^{+}CD44^{+}CD90.2^{+}$) all populations were cultured under identical conditions for a similar passage number prior to extensive phenotypic and functional characterisation. We report a high level of concordance with respect to morphology, growth properties, cell surface proteins, gene expression profile and multipotentiality *in vitro* between these three populations. Our data support a common phenotype for distinct organ-specific MSCs, reinforcing the hypothesis that such cells are involved in tissue maintenance and repair [28]. However, we also report variations in the level of epitope presentation and distinct phenotypic signatures, supporting the concept of molecular ‘memory of tissue origin’ and the existence of distinct functional roles for MSC-like cells isolated from different tissues.

Results

The colony forming assay represents an accepted and robust selection for a specific stem cell-like population (3,4). CFU-F cultures are known to contain stem cells that are self-renewing but also able to give rise to more committed progenitors through asymmetric division. They may also contain a few differentiated offspring with time. While the ultimate cultures are not homogeneous, short term proliferating cells are purged from the cultures by continued passage. In order to directly compare MSC-like cells from a variety of tissue sources, we initially derived colony forming unit-fibroblast (CFU-F) populations from total adult murine bone marrow, heart and kidney as described in Supplementary Data. All cells analysed in this comparative study were plated in αMEM + 20% FCS and subsequently cultured as adherent cells for a similar number of passages prior to further characterization and functional analysis (Figure 1A). An initial immunophenotyping for cell surface epitopes considered characteristic of MSCs suggested that all cultures displayed a $Sca1^{+}CD29^{+}CD44^{+}$ and $CD11b^{-}CD31^{-}CD45^{-}CD117^{-}$ phenotype, verifying the MSC nature of all three populations (Supplementary Figure S1).

Comparative phenotype and comprehensive immunophenotypic analysis.

All three populations were plastic-adherent and displayed similar fibroblast-like morphologies (Fig. 1Ba-c). Cells from all populations had a similar appearance with each population showing heterogeneity of cell size, large often peripherally-located nuclei with dense chromatin and a large amount of granular cytoplasm (Fig. 1Bd-f). Cells varied in size from 20-120 μm. Murine bmMSC, cCFU-F and kCFU-F were all able to differentiate along mesodermal lineages *in vitro* when cultured under adipogenic, osteogenic or chondrogenic conditions (Fig. 1Bg-o) although cCFU-F showed less robust formation of chondrocyte pellets and were slower to induce adipocyte differentiation.

The immunophenotype of all three populations was comprehensively compared using a panel of 81 PE-conjugated antibodies (Supplementary Table S1). A heat map showed extensive congruence in the percentage of cells positive for a given CD epitope between the three populations, although hierarchical clustering revealed that bmMSC and kCFU-F were more similar to each other than to cCFU-F (Figure 2A). An examination of all epitopes detected on >20% of cells in at least one of the three populations (Figure 2B) highlighted a number of matrix and adhesion molecules, potentially reflecting niche molecules expressed in common. These included CD29, CD44, CD49e, CD51, CD61, CD81 and CD24. CD105 (endoglin), a marker of primitive haematopoietic stem cells (HSCs), was also expressed on a high proportion of all cells. The expression of CD markers associated with immune regulation, including CD24, CD80, CD81 and CD90.2, implies a common immune regulatory function for MSC in multiple organs. CD49e, CD51, CD71 and CD105 have been previously reported on human MSC [28]. CD73, generally accepted as a diagnostic human MSC marker, [1, 5], was not present on a significant percentage of any murine population analysed in this study (Supplementary Table 2). Conversely, CD80, negative on human MSC, was found on all 3 populations of murine MSC. Of note, while cCFU-F were isolated as GFP+ cells from a PDGFRα-GFP mouse strain, the mean percentage of cCFU-F cells positive for CD140a (detects PDGFRα) was 12%, comparable to the levels seen in both other populations. Analysis of the GFP positivity on FITC channel during immunophenotyping showed 23.7% GFP^+ cells. This variation from the antibody may result from perdurance of the GFP. (Data not shown).

Gene expression profiling reveals considerable congruence between the three populations.

To further compare phenotypes, Illumina microarray expression profiling was performed on RNA isolated from the three populations. Analysis of expression of >45,000 transcripts showed that 81.1% of genes were expressed to some degree across the combined set of samples. Pearson correlations of pair-wise comparisons revealed r^2 values ranging from 0.878 to 0.924 (Figure 3A). This represents a very high level of similarity between the three cell types, although bmMSC were again more similar to kCFU-F than to cCFU-F. We ranked all genes in order of level of expression for all three populations. Ninety-five of the top 100 bmMSC-expressed genes were also ranked within the top 250-ranked genes listed for the other populations (Supplementary Table 4). As expected, most of the top 100 genes encoded house-keeping proteins. However, this list also included regulatory molecules and secreted proteins involved in tissue remodelling, repair and inflammatory modulation. Among the most highly expressed genes in all lines was *Zyxin*, *Thymosin β10* and *Macrophage inhibitory factor* (*MIF*) (Supplementary Table 4). *Zyxin* (ranked 1 for cCFU-F, 10 for kCFU-F and 35 for bmMSC) encodes a member of the LIM domain family of focal adhesion adaptor proteins that is likely to also serve as a component of transcription factor complexes. Thymosin β10, a monomeric actin-sequestering protein, is secreted and has paracrine functions in wound repair [29], vasculogenesis [30], inflammation and cancer [31, 32]. In contrast to its paralogue thymosin β4, which is pro-angiogenic, thymosin β10 inhibits angiogenesis. MIF protein has emerged as a major inflammatory mediator through its chemokine-like functions, acting both upstream and downstream of inflammatory inducers. It has been proposed as a "master regulator" for leukocyte chemotaxis and arrest. MIF is also pro-angiogenic and inhibits migration and division of smooth muscle (SM) cells. Other commonly expressed secreted products included biglycan, a proteoglycan that modulates cellular proliferation and migration; serpinh1/HSP47, a procollagen chaparone involved in collagen remodelling and formation of scar tissue; serpinf1/PEDF, an inhibitor of endothelial cell proliferation and

migration while also acting as a fibroblast chemoattractant; Sparc/Osteonectin, an MMP-activated, collagen-binding protein implicated in collagen fibril and basal lamina formation; and CTGF/CCN2, a known mediator of tissue fibrosis. These all strongly reflect the fibroblastic phenotype of these cells. Pathway analysis of genes expressed in common between these MSC populations identified genes involved in immunity, cell adhesion, BMP signalling, chemokine signaling, homeodomain transcription factors, metalloproteinases and their TIMP inhibitors (Table 1).

Microarray data was validated using quantitative PCR (qPCR). This was first performed on a set of genes chosen for their wide variation in gene expression between the three cell types (*Prl2c2,GHR, Zyx, Des*) (Supplementary Figure S2). qPCR was then performed to validate the expression of genes regarded as classical MSC [25, 26] and/or pericyte markers [28, 33] (*Twist1, CCL7, MMP2, MIF, HoxA5, Tagln*) [34] (Supplementary Figure S3). This demonstrated good validation of relative expression levels between microarray and qPCR.

Enrichment for stem cell networks in all three MSC-like populations

To investigate the stem cell nature of these three populations, the expression of murine orthologs of components of the recently described Plurinet was examined in these cell lines [34]. Murine orthologs of the human plurinet genes were examined for their mean normalised expression and 66% of these orthologs displayed an Illumina detection score >0 in at least one population (Supplementary Table 6). In addition, hierarchical clustering showed strong congruence between the three CFU-F populations (Figure 3B). Once again, a closer relationship was evident between bmCFU-F and kCFU-F. Figure 3C illustrates the subcellular localisation and network relationships of those Plurinet genes expressed by these populations and qPCR was used to validated these results for a subset of Plurinet genes detected as present

in the three populations (*Myc*, *AnxA2* and *Smarcad1*) (Supplementary Figure S4). We also investigated the expression of genes critical for induced pluripotency. Expression of *Klf4* and *Sox2* (not in the Plurinet), while above the threshold for detection by microarray, was very low (Supplementary Figure S4). Expression of both *Nanog* and *Oct4* (*Pou5f1*) fell below the Illumina detection threshold for all cell lines. qPCR for these genes also indicated extremely low levels of mRNA (Supplementary Figure S4). Despite this, the extensive expression of other Plurinet genes implies an active stem cell state in all three MSC-like populations.

Immunosuppressive capacity of bmMSC, cCFU-F and kCFU-F

bmMSC have long been known to be immunomodulatory, affecting the proliferation and phenotype of T-cells, B-cells, NK cells and antigen-presenting cells through a cytokine/chemokine cascade [35]. Lacking MHC Class II, they are also immunoprivileged in an allogeneic setting, leading to the concept of an "off-the-shelf" therapy for regenerative medicine. Given the molecular and immunophenotypic evidence for considerable congruence between these three populations, we assessed the *in vitro* capacity of each population to suppress T-cell proliferation when added to a mixed lymphocyte reaction using LPS-stimulated allogenic T-cells as responders (Fig. 4A). bmMSC were suppressive at both low and high numbers of cells added (MSC:responder ratios 1:100 and 1:10, respectively). kCFU-F were only significantly suppressive using the higher number of cells. In contrast, cCFU-F were not suppressive with either cell number. This was confirmed in a "third party" MLR in which cCFU-F, donor and responder lymphocytes were all mismatched for MHC. In this setting, cCFU-F in fact increased responder T-cell proliferation (data not shown), suggesting a possible pro-survival effect [36].

Correlating differences in gene expression with functional behaviour.

Given this functional difference between the populations, hierarchical clustering was performed on a set of 6487 genes shown to be differentially expressed between the 3 populations (Figure 4B). The number of genes differentially expressed ($B>0$, $p<0.005$) between bmMSC and kCFU-F was 2746, with 3535 between cCFU-F and kCFU-F and 4572 between bmMSC and cCFU-F (Figure 4C). We then identified genes in which expression was differentially higher or lower in one of the three populations versus the remaining two (Figure 4D,E). Genes up-regulated in one population represent genes enriched in or specific to a given cell type (Figure 4D). These genes are listed in Supplementary Table 7A, C and E. We have defined specific markers of each cell population as those genes for which expression in the population of interest was >500RFU, expression in the comparative populations was <200RFU and the fold difference greater than 5. Table 2 lists the 5 most population-specific genes. Genes that were differentially under-expressed in a given cell type were also identified (Figure 4E, Supplementary Table 7B, D, F). Genes underexpressed in bmMSC represent genes commonly enriched in the two solid tissue-derived MSC populations.

Organ-specific gene expression signatures in MSC-like populations

Observed differences in gene expression between these three populations should inform our understanding of functions enhanced in one organ but reduced in others, unique organ-specific functions, and potentially features that relate to the cellular or developmental origins of organ-specific CFU-F ("memory of tissue origin"). In the case of kCFU-F, the enriched expression of *Mylk*, *Myom*, *Desmin* and *Serpinb2* (Supplementary Table 7C) suggest a strong relationship with the perivascular and mesangial cells of the kidney, in keeping with the proposed perivascular origin for MSC [4, 13]. As well as mesangial cells, *Mylk* and *Myom1* are expressed in smooth muscle, as is *Myh11*, a gene expressed equivalently in cCFU-F and kCFU-F but not in bmMSC. This may again reflect a perivascular location due to the more

established arterio-venous circulation present in solid organs. No evidence was found for the derivation of kCFU-F from the nephron epithelia. kCFU-F also differentially express *Nestin*. This gene is expressed in a number of stem cell populations and has been proposed as a marker of multipotent progenitors [37]. *Nestin* expression has been reported in mesangial cells, endothelial cells and podocytes of the kidney, where its expression increases in response to glomerular injury. It has also been shown to mark a population of papillary interstitial cells [38] whose distribution within the kidney shifts from the medulla to the cortex in response to acute renal ischaemia [39]. This may imply an organ-specific role for these cells in normal tissue turnover.

For cCFU-F, analysis of differential gene expression implied a possible 'memory of tissue origin'. The gene encoding the MADS box transcription factor, *Mef2c*, essential for deployment of cardiac progenitor cells to the forming heart [40], was cCFU-F specific and expressed 6.6-fold and 66 fold over kCFU-F and bmMSC levels, respectively. An enhancer responsible for cardiac *Mef2c* expression is regulated by the LIM homeodomain factor ISL1, which is often used to define cardiac progenitor cells in the embryo and adult [41]. Whilst *Isl1* fell just short of the criteria for tissue-specificity, it was nonetheless expressed 45-fold and 33-fold above the low levels seen in kidney and bmMSC, respectively. T-box genes also play a major role in heart development, and *Tbx4* was identified here as cCFU-F-specific. While not itself expressed in the developing heart, *Tbx4* is a paralogue of *Tbx5*, which participates in the core cardiac transcription factor gene network and is mutated in Holt-Oram (hand/heart) syndrome in humans [42]. Tbx4 induces the fibroblast growth factor 10 gene (*Fgf10*) in limb patterning [43] and *Fgf10* was also cCFU-F-specific. Other genes involved in transcription, cell shape, migration, growth and differentiation (*Barx1*, *Ednrb*, *Gpr88*, *Ramp3*, *Gas7*,

Mapk13, Mmp3, Sema3F/5F), were also enriched in cCFU-F, perhaps identifying unique functions or adaptations of cCFU-F.

The bmMSC population showed strong enrichment for *Meox1* (10-fold up-regulated in bmMSC), a transcription factor associated with formation of somites and maintenance of axial skeleton formation [44, 45]. This may reflect 'memory of the tissue of origin' or represent the presence of a subpopulation of more primitive cells. A striking number of immune-related genes were also found to be either specific to, or enriched in, bmMSC (Supplementary Table 7). While many of these appear to be involved in innate immunity (*Oas1g, Oasl2, Ccl9, Cxcl10, Granzyme D/E* and *Dhx58*), they are not known to influence T-cell proliferation in the assay used here. While the up-regulation of these genes implies an active stress response pathway, or even the initiation of a viral response, other genes indicative of such a response, such as *MHC class I (H2)* and *IFNα/γ,* were not more highly expressed in bmMSC.

Dissecting functional differences between MSC-like populations at the level of protein.

While immunophenotypically similar at the level of the percentage of the population positive for a given epitope, we investigated whether the observed functional variability between populations resulted from differences in the prevalence of individual cell surface epitopes. This was possible because the immunophenotyping was performed using PE conjugated antibodies (one PE fluorophore per antibody), enabling an estimation of relative epitope density by comparing mean fluorescence intensity between populations. Overall this analysis highlighted a reduction in epitope density on the cCFU-F population, a population that showed little immunosuppressive activity and potentially reduced multipotency. For 25/81 antibodies, mean intensity was >20 fold above background in at least one population (Figure

5A), however this included only 5 antibodies present on >20% of the cells in those populations. Conversely, of the six epitopes for which >50% of cells in all population were positive, three antigens in particular showed considerable variability in epitope density (CD49e, CD81 and Sca1) (Figure 5B). kCFU-F showed a lower receptor density of Sca1 compared to bmMSC. cCFU-F showed a generalised reduction in epitope density for all epitopes apart from CD24 and CD90.2. In the case of CD24, cCFU-F showed both the highest percentage (95.35% Figure 2B) and epitope density (11.8 fold compared to 6.2 fold for bmMSC and 4.7 fold for kCFU-F, Supplementary Table 2) of all three populations whereas for CD90.2, while only 1.1% of cCFU-F cells were positive (Figure 2B), they showed the highest mean relative fluorescence intensity compared to bmMSC and kCFU-F (Figure 5A). A number of minor subpopulations existed within which the cells displayed tissue-specific enrichment for epitope density (Supplementary Tables 2,3). kCFU-F showed a very small subpopulation (1.55%) of cells differentially positive for the chemokine receptor CXCR4 (CD184) (42.5 fold) and another small subpopulation (1%) differentially positive for CD41 (Integrin alpha-IIb) (70.8 fold) with respect to bmMSC or cCFU-F (Supplementary Tables S2, S3).

Correlations between gene expression and immunophenotyping.

While there is no guarantee of a direct correlation between mRNA levels and protein, as not all mRNA is present at the translational machinery and different cell surface proteins show different rates of delivery to and recycling from the plasma membrane, this study did provide a unique opportunity to directly compare gene expression data with immunophenotyping. This provided several challenges. Not all CD epitope-encoding genes were represented on the microarray. The amount of protein present will depend upon both the number of cells carrying the protein and how many copies are present per cell (combination of percentage positive and

relative epitope density). Finally, some microarray oligonucleotides match alternate transcripts or map to multiple sites in the genome. To overcome this, we examined the relative fluorescence for all oligos representing genes that encoded CD epitopes present on >40% of any given population. In this way, we were able to confirm the expression of 11/13 of these epitopes (Figure 5C, Supplementary Table 8) with the remaining falling below the Illumina detection limit. Despite the overall dimness of the cCFU-F for most epitopes, those that were present on >40% of cCFU-F showed levels of gene expression comparable to both bm-MSC and kCFU-F, suggesting that cCFU-F either showed greater recycling of epitopes from the cell surface, reduced translation or a reduction in delivery to the plasma membrane.

Discussion

It has previously been shown, based on cell surface immunophenotype and mesodermal differentiation capacity, that MSC-like cells reside in many postnatal organs in mice [14]. Our findings support the notion that MSC-like populations from diverse organs, isolated based on a capacity to form CFU-F, share morphological and molecular characteristics as well as multipotency in common with archetypal bmMSC [46]. Our results show high congruence in gene expression, mesodermal potential and immunophenotype. However, embedded in the detectable differences were expression patterns that support the hypothesis that tissue-specific MSC populations are distinct and retain a 'memory of tissue origin' reflective of their unique ontogeny and functional roles.

This is not the first report describing MSC-like populations from adult organs. Several groups have previously compared the transcriptional profiles of MSC populations from bone marrow, amniotic fluid, amniotic membrane and umbilical cord blood and compared these to fetal organs, including developing heart and kidney [27, 47]. As we observed in our studies, such studies reported *Ctgf, CD44, S100* genes encoding calcium binding proteins (*S100a6* in their study and *S100a11* in ours), serpin peptidase inhibitor genes (*Serpine1* versus *Serpinh1* and *Serpinf1*) and annexins (*Anxa1* versus *Anxa2*) as some of the most highly expressed genes common to all sources of MSC. However, other genes previously linked to MSC were only selectively over-expressed in specific populations in this study. For example, kCFU-F showed differential over-expression of *Hoxb6* and *Anxa1* whereas cCFU-F showed differential over-expression of *Agtr1b*.

MSC are reported to be able to home to distant sites of damage and participate in tissue repair and regeneration. This occurs in response to adhesion molecules, cytokines and chemokines,

presumably via a mechanism not dissimilar to that required to initiate leukocyte rolling and diapedesis [48]. Our immunophenotyping analysis showed significant expression of CD29 (integrin β1), CD49e (integrin α5), CD51 (integrin αV) and CD44, all of which are likely to play a role in cell-cell adhesion during active homing. Of note, CD61 (integrin β3) was only detected on bmMSC and kCFU-F. The expression data revealed marked expression of *Mmp2, Mmp13* and *Mmp24* and their inhibitors *Timp1, Timp2* and *Timp3* in all three cell types. The balance between MMP and TIMP is crucial in allowing MSC to migrate through basement membrane and endothelium to reach a distant sight of injury. It has been recently reported that *Mmp/Timp* expression by MSC can be mediated by inflammatory cytokines. Such compounds may also regulate the mobilisation of these populations from perivascular locations *in vivo* when required for localized tissue repair [49, 50].

Many immunity-associated genes previously linked to MSCs were also expressed by all 3 cell populations, particularly by bmMSC. A comparison of the functional capacity of each population to influence lymphocytic proliferation suggested significant differences between the three sources of cells, with cCFU-F showing little activity. This has also been observed in a previous study of MSC-derived populations from fetal heart [51], although the converse has also been reported [52]. We re-examined the cell surface immunophenotype of these three populations in order to identify an underlying mechanism for such functional variability. While all three populations showed high percentages of cells positive for CD81, the relative mean intensity of this epitope on cCFU-F was dramatically lower than in either of the other populations. CD81 (TAPA-1) is a member of the transmembrane 4 superfamily whose loss has been associated with enhanced T-cell proliferation [53]. It has been proposed that MSCs mediate their humoral properties via the secretion of membrane-bound exosomes that contain a variety of chemokines and have been reported to contain CD81 [54]. The delivery of such

exosomes can reduce infarct size in animal models [54], suggesting a potential role for CD81 in immunosuppression. Hence, reduced CD81 may at least in part explain the reduced immunosuppressive capacity of the cCFU-F population.

Several studies [55-58] have reported the expression of embryonic stem (ES) cell markers on MSC derived from bone marrow, adipose, dermal and heart. Knockdown of *Oct4* in MSCs removes them from the cell cycle, as may be the role for this protein in ES cells. However, not all studies show *Oct4* expression in MSC and our data suggests no/ negligible expression of this gene. However, we did observe expression of a large number of Plurinet genes in these MSC populations. This may indicate a closer alignment to the 'attractor state' of pluri / multipotency than other adult cell populations. Indeed MSCs from a variety of sources are more readily reprogrammed to a pluripotent state than fibroblasts [59, 60].

The proposed association between organ-specific MSC populations and the pericytic/ perivascular compartment agrees with literature from over 50 years ago addressing the potency and plasticity of pericytes and their related lineages [61]. MSCs and pericytes likely share a common phylogenetic and possibly ontological relationship being descendant of distinct vascular beds both during embryo development but also in the adult [62], and in the vasculature of tumours [63]. It has been suggested that within the perivascular environment, a continuum exists between fibroblasts, myofibroblasts and vascular smooth muscle cells and that pericytes and MSC-like populations are closely related and located adjacent to the vascular endothelium throughout the organs of the body. In humans, both MSC and pericytes express CD146, CD140b, CD271 and NG2 suggesting considerable commonality between these cell types [13, 28, 33, 64, 65]. In support of this, we found gene and/or protein expression of CD146, CD140b, *αSMA*, *Cspg4/ NG2*, CD24, *Annexin A5*, and *Desmin* in each

of our 3 MSC-like populations. The relative level of each marker did vary, potentially indicating differences in the cell of origin or position along a lineage continuum of each population, the latter again potentially being affected by population heterogeneity. Analysis of the most compartment-specific genes for each population particularly supported this hypothesis for the kCFU-F with enriched expression of *Myh11, Mylk, Mcam (CD146), Efnb2, Edn1, Angpt2* and *Vegfc* (Suppl Table S7C), all of which are associated with vascular, lymphatic or perivascular smooth muscle development. In addition, both kCFU-F and cCFU-F differentially expressed *Crim1*, a transmembrane regulator of VEGF activity that is known to be expressed in the perivascular musculature of large arteries [66]. The stronger link with this ontogeny and MSC-like fractions isolated from solid organs may be of significance.

One of the major challenges to the application of MSCs to organ regeneration and repair *in vivo* has been cell delivery. While it has been shown in some studies that MSCs delivered into the circulation can home to sites of damage, including sites of ischemic injury in the kidney, the mechanism of migration is still unclear and there is substantial loss of cells delivered via this approach [48]. To fulfil the promise of MSC-mediated tissue repair, it may therefore prove necessary to stimulate the endogenous organ-specific MSC populations. Our data on the patterns of differential gene expression between populations provide supporting evidence for a 'memory of tissue origin', highlighting a key gap in our understanding of CFU-F/MSC biology and the potential of these cells for tissue repair. Most notable here was the link between cCFU-F and key developmental transcriptional networks, including *Mef2c* and *Isl1*. Such tissue-specific signatures may be derivative of the stem cell or more differentiated components of the colonies. These may be related in evolutionary or ontological origin and share a common set of functions, yet nonetheless possess differentiative potential and/or cellular functions atuned to their specific roles in the tissue of origin. The other explanation

for such differential gene expression in specific MSC populations would be contamination of the cultures with organ-specific cell types. The derivation of these MSC populations from CFU-F, followed by passaging, would make it unlikely that such residual heteroegeneity is the primary cause of differential gene expression unless these 'contaminating' subpopulations were able to proliferate with a similar phenotype to MSCs. The functional pertinence of such tissue-specific phenotypes will require additional functional investigation, but may be critical to conferring organ-specific regenerative capacities on organ-specific populations.

In conclusion, this study has expanded our understanding of the commonalities in genotype, phenotype and function of murine MSC-like cells of distinct tissue origin. This has served to further reinforce the concept of a common perivascular continuum and the retention of organ-specific roles. Further functional understanding of both the similarities and differences between such organ-specific populations will be crucial to the development of future cellular therapeutic approaches to tissue repair as these results suggest that finding the best "MSC" for a particular clinical application will be of paramount importance.

Materials and Methods

Isolation and *ex vivo* expansion of MSC-like populations

All procedures were approved by the University of Queensland or the St. Vincent's Hospital/Garvan Institute Animal Ethic Committees. All MSC populations were derived from mice of the C57BL/6 strain. Bone/bone marrow MSC (bmMSC) were isolated from crushed bones as described in Supplementary Data. Both cardiac and kidney MSC populations represent populations able to be cultured as colony forming unit-fibroblast (CFU-F) cultures [3] although each were isolated based upon specific protocols devised for heart or kidney respectively, as described in Supplementary Data. Each biological replicate represented an independently initiated culture. In the case of cCFU-F, a single culture represented a single heart with each heart able to generate approximately 17000 CFU-F colonies. In the case of kidney, one biological replicate represents isolation from a single animal (two kidneys), which equates to approximately 3-5000 colonies. As bmMSC was isolated from crushed bones and not simple bone marrow aspirates, a single replicate represented the pooled crushed bones of 6-8 animals. Due to the capacity for $CD45^+$ leucocytes to be propagated along with bmMSC, cultures once established were FACS sorted to remove $CD45^+$ cells.

All three cell types were cultured in αMEM (Invitrogen) + 20% FCS for up to 14 passages. Microarray expression profiling and initial immunophenotyping was performed at passage 5 to 10 (kidney P5, heart P7, bm P10). Initial immunophenotyping was performed with Sca1, CD11b, CD29, CD31, CD34, CD44, CD45, CD90.2 and CD117 to establish that they displayed an MSC-like phenotype (Supplementary Figure 1). Subsequent characterization included morphological analysis and mesodermal differentiation assays (Figure 1), performed as described in Supplementary Data.

CD antibody array immunophenotyping

A total of 81 R-Phycoerythrin (PE)-conjugated CD antibodies were used to examine the immunophenotype of each cell type. A list of all antibodies used and the protein epitopes they recognise can be found in Supplementary Table S1. Antibodies were sourced from BD Biosciences and eBioscience. bmMSC, cCFU-F and kCFU-F were cultured until 70-80% confluent and dissociated from flasks with TrypLE Select (Invitrogen), washed with PBS and $5x10^6$ cells were resuspended in PBS + 2% BSA. $5x10^4$ cells were transferred to each well in a V-bottom 96 well plate and incubated with a 1:100 dilution of anti-mouse PE-conjugated antibodies. Plates were incubated on ice for 30 min, centrifuged at 1000 rpm, 5 min, 4˚C, washed in PBS + 1% BSA, fixed in 4% PFA, 15 min on ice before being washed and resuspended in PBS. Samples were analysed using BD Bioscience LSRII with microplate reader attachment. Percentage positive cells (gating relative to unstained negative control) and mean fluorescence intensity data were calculated using BD FACSDiva software (v 6.1.2). Histogram overlays of representative results were created using Walter and Eliza Analysis Software: Eclectic and Lucid (WEASEL, V2.7.4, Walter and Eliza Hall Institute for Medical Research, Melbourne, Australia). Tree graphs were created in R software (v 2.6.2; http://www.r-project.org/) [67]. Initial experiments using the Violet Viability kit (Invitrogen) were used to define a region encompassing viable cells on Forward Scatter Area versus Side Scatter Area dotplot. This was applied to subsequent analysis where the dye was not used (data not shown). Positive populations were delineated based upon gating to exclude non-stained internal negative controls included in each series of biological replicates (two non-stained control per dataset). The same gate was applied to all epitopes analysed in each replicate. The percentage of cells positive represents the percentage of the counts present within the positive gate. Mean fluorescence intensity indicates the mean fluorescence for all

cells within the positive cell gate. The average of these values for each cell type is tabulated in Supplementary Table 3. Relative intensity for different epitopes (equivalent to epitope density) within a given biological replicate was calculated by normalising mean fluorescence intensity back to the mean fluorescence intensity of the unstained negative control samples, arbitrarily set at 1.0. This was expressed as fold change relative to no stain (see Supplementary Table 2). A direct comparison between immunophenotypic data obtained using the protocol adopted in the screen with the conventional FACs performed in the initial immunophenotyping is presented in Supplementary Figure S5.

Microarray sample preparation and data analysis

Detailed microarray sample preparation and analysis methods can be found in the Supplementary Data. Briefly, biological replicates included cells cultured to 65-80% confluence in 4 separate flasks concurrently for all three cell types. The same batch of αMEM and FCS was used for all cells and handling was carried out on all cells simultaneously to minimize transcriptional noise. Biotin-labelled cRNA was hybridized to mouse WG6 v2 array (Illumina Inc, San Diego, CA) at 55ºC for 18 h, followed by labelling with streptavidin-Cy3 (GE Healthcare). Arrays were scanned with the BeadStation 500 System and raw probe expression values were extracted using BeadStudio v3 software (Illumina). The complete microarray data can be found in the publicly accessible GEO database (Accession number to be supplied). Further details of data analyses are described in Supplementary Data. In brief, raw probe expression values were imported in R software (version 2.6.2) [67], background corrected and quantile normalized using the Lumi package [68]. Using the LIMMA package [67], an Empirical Bayes Analysis was run to determine the genes with significant differential expression between each of the three cell types. This analysis included a multiple testing

correction to reduce false positives [69]. For each pair-wise comparison genes with a B-score greater than 0 were selected as significant ($p<0.005$).

In order to measure the similarity between the three cell types, Pearson correlations of each cell type against each other were calculated (r^2). The correlations were based on a subset of genes with medium to high expression levels selected using Illumina's Detection Score (20,662 genes). Ingenuity Pathway Analysis (Ingenuity Systems Inc., Redwood City, CA) was performed to categorize the differentially regulated genes.

When comparing gene expression with protein levels of CD epitopes, all oligonucleotides designated as representing a given CD epitope encoding gene were mapped back to the UCSC mouse genome build to check for oligonucleotides that mapped to multiple locations in the genome (multimappers), alternative isoforms or the wrong locus. Data from oligonucleotides was also excluded from the comparison if the expression of that oligonuclotide was regarded as below background as determined by an Illumina detection score of >0.

Mixed leukocyte reaction (MLR) assay

Mixed lymphocyte reaction assays were performed as previously described [70]. bmMSC, cCFU-F and kCFU-F were plated at 3000 or 30 000 cells per well in a U-bottom 96 well plate (Greiner, Kremsmünster, Austria) in αMEM + 20% FCS overnight and then irradiated (2000 cGy) prior to co-culture. Assays were carried out in complete media (αMEM, 10% FCS, β-mercaptoethanol, HEPES and P/S/G). Stimulator splenocyte cells from BALB/c mice were cultured overnight with 100 ng/ml lipopolysaccharide (LPS, Sigma-Aldrich) in culture media in a humidified 37°C, 5% CO_2 incubator, then irradiated (2000 cGy) prior to co-culture [70]. Responder T-cells derived from C57BL/6 mice were purified using a pan T-cell isolation kit

(Miltenyi Biotec, Gladbach, Germany). Stimulator cells ($2x10^5$ cells/well) and responder T-cells (3×10^5 cells/well) were co-cultured (complete αMEM) in a humidified 37°C, 5% CO_2 incubator. Proliferation was assessed by [^{3}H]-thymidine incorporation (1 μcurie/well) (GE Healthcare) after a total of 96 h of culture. Cells were harvested using the TOMTEC 96-well Mach III Harvester (Perkin-Elmer, Victoria, Australia) and counts per minute (cpm) measured on a 1450 MICROBETA TRILUX β-scintillation counter (Perkin-Elmer).

Acknowledgements

This work was supported by the Australian Stem Cell Centre (grants to K.A., M.L, R.H. and S.G.) the Mater Medical Research Institute/ Mater Foundation (KA) and NHMRC (AMR). The microarray research was supported by the Australian Research Council Special Research Centre for Functional and Applied Genomics (Institute for Molecular Bioscience) Microarray Facility. Technical assistance in immunophenotyping was provided by John Wilson and Virginia Nink from the Queensland Brain Institute Flow Cytometry Facility, University of Queensland. Further technical assistance was supplied by Robert Wadley. AMR is a Queensland Government Smart Futures Fellow. ML and SG are Research Fellows and RH is an Australia Fellow with the National Health and Medical Research Council, Australia.

References

1. E.M. Horwitz, K. Le Blanc, M. Dominici, I. Mueller, I. Slaper-Cortenbach, F.C. Marini, R.J. Deans, D.S. Krause, A. Keating, Clarification of the nomenclature for MSC: The International Society for Cellular Therapy position statement, Cytotherapy. 7 (2005) 393-395.

2. M.F. Pittenger, A.M. Mackay, S.C. Beck, R.K. Jaiswal, R. Douglas, J.D. Mosca, M.A. Moorman, D.W. Simonetti, S. Craig, D.R. Marshak, Multilineage potential of adult human mesenchymal stem cells, Science. 284 (1999) 143-147.

3. A.J. Friedenstein, U.F. Deriglasova, N.N. Kulagina, A.F. Panasuk, S.F. Rudakowa, E.A. Luria, I.A. Ruadkow, Precursors for fibroblasts in different populations of hematopoietic cells as detected by the in vitro colony assay method, Exp Hematol. 2 (1974) 83-92.

4. P. Bianco, P.G. Robey, P.J. Simmons, Mesenchymal stem cells: revisiting history, concepts, and assays, Cell Stem Cell. 2 (2008) 313-319.

5. M. Dominici, K. Le Blanc, I. Mueller, I. Slaper-Cortenbach, F. Marini, D. Krause, R. Deans, A. Keating, D. Prockop, E. Horwitz, Minimal criteria for defining multipotent mesenchymal stromal cells. The International Society for Cellular Therapy position statement, Cytotherapy. 8 (2006) 315-317.

6. M. Kassem, M. Kristiansen, B.M. Abdallah, Mesenchymal stem cells: cell biology and potential use in therapy, Basic Clin Pharmacol Toxicol. 95 (2004) 209-214.

7. L. da Silva Meirelles, N.B. Nardi, Murine marrow-derived mesenchymal stem cell: isolation, in vitro expansion, and characterization, Br J Haematol. 123 (2003) 702-711.

8. S.S. Wang, S. Asfaha, T. Okumura, K.S. Betz, S. Muthupalani, A.B. Rogers, S. Tu, S. Takaishi, G. Jin, X. Yang, D.C. Wu, J.G. Fox, T.C. Wang, Fibroblastic colony-forming unit bone marrow cells delay progression to gastric dysplasia in a helicobacter model of gastric tumorigenesis, Stem Cells. 27 (2009) 2301-2311.

9. Y. Ebihara, M. Masuya, A.C. Larue, P.A. Fleming, R.P. Visconti, H. Minamiguchi, C.J. Drake, M. Ogawa, Hematopoietic origins of fibroblasts: II. In vitro studies of fibroblasts, CFU-F, and fibrocytes, Exp Hematol. 34 (2006) 219-229.

10. J.K. Fraser, I. Wulur, Z. Alfonso, M. Zhu, E.S. Wheeler, Differences in stem and progenitor cell yield in different subcutaneous adipose tissue depots, Cytotherapy. 9 (2007) 459-467.

11. S.A. Steigman, D.O. Fauza, Isolation of mesenchymal stem cells from amniotic fluid and placenta, Curr Protoc Stem Cell Biol. Chapter 1 (2007) Unit 1E 2.

12. R. Sarugaser, D. Lickorish, D. Baksh, M.M. Hosseini, J.E. Davies, Human umbilical cord perivascular (HUCPV) cells: a source of mesenchymal progenitors, Stem Cells. 23 (2005) 220-229.

13. M. Crisan, S. Yap, L. Casteilla, C.W. Chen, M. Corselli, T.S. Park, G. Andriolo, B. Sun, B. Zheng, L. Zhang, C. Norotte, P.N. Teng, J. Traas, R. Schugar, B.M. Deasy, S. Badylak, H.J. Buhring, J.P. Giacobino, L. Lazzari, J. Huard, B. Peault, A perivascular origin for mesenchymal stem cells in multiple human organs, Cell Stem Cell. 3 (2008) 301-313.

14. L. da Silva Meirelles, P.C. Chagastelles, N.B. Nardi, Mesenchymal stem cells reside in virtually all post-natal organs and tissues, J Cell Sci. 119 (2006) 2204-2213.

15. L. Iop, A. Chiavegato, A. Callegari, S. Bollini, M. Piccoli, M. Pozzobon, C.A. Rossi, S. Calamelli, D. Chiavegato, G. Gerosa, P. De Coppi, S. Sartore, Different cardiovascular potential of adult- and fetal-type mesenchymal stem cells in a rat model of heart cryoinjury, Cell Transplant. 17 (2008) 679-694.

16. M.G. Roubelakis, K.I. Pappa, V. Bitsika, D. Zagoura, A. Vlahou, H.A. Papadaki, A. Antsaklis, N.P. Anagnou, Molecular and proteomic characterization of human mesenchymal stem cells derived from amniotic fluid: comparison to bone marrow mesenchymal stem cells, Stem Cells Dev. 16 (2007) 931-952.

17. P.V. Guillot, C. Gotherstrom, J. Chan, H. Kurata, N.M. Fisk, Human first-trimester fetal MSC express pluripotency markers and grow faster and have longer telomeres than adult MSC, Stem Cells. 25 (2007) 646-654.

18. Z.Y. Zhang, S.H. Teoh, M.S. Chong, J.T. Schantz, N.M. Fisk, M.A. Choolani, J. Chan, Superior osteogenic capacity for bone tissue engineering of fetal compared with perinatal and adult mesenchymal stem cells, Stem Cells. 27 (2009) 126-137.

19. P.V. Guillot, C. De Bari, F. Dell'Accio, H. Kurata, J. Polak, N.M. Fisk, Comparative osteogenic transcription profiling of various fetal and adult mesenchymal stem cell sources, Differentiation. 76 (2008) 946-957.

20. G. Li, X.A. Zhang, H. Wang, X. Wang, C.L. Meng, C.Y. Chan, D.T. Yew, K.S. Tsang, K. Li, S.N. Tsai, S.M. Ngai, Z.C. Han, M.C. Lin, M.L. He, H.F. Kung, Comparative proteomic analysis of mesenchymal stem cells derived from human bone marrow, umbilical cord, and placenta: implication in the migration, Proteomics. 9 (2009) 20-30.

21. J.J. Montesinos, E. Flores-Figueroa, S. Castillo-Medina, P. Flores-Guzman, E. Hernandez-Estevez, G. Fajardo-Orduna, S. Orozco, H. Mayani, Human mesenchymal stromal cells from adult and neonatal sources: comparative analysis of their morphology, immunophenotype, differentiation patterns and neural protein expression, Cytotherapy. 11 (2009) 163-176.

22. S. Barlow, G. Brooke, K. Chatterjee, G. Price, R. Pelekanos, T. Rossetti, M. Doody, D. Venter, S. Pain, K. Gilshenan, K. Atkinson, Comparison of human placenta- and bone marrow-derived multipotent mesenchymal stem cells, Stem Cells Dev. 17 (2008) 1095-1107.

23. D. Noel, D. Caton, S. Roche, C. Bony, S. Lehmann, L. Casteilla, C. Jorgensen, B. Cousin, Cell specific differences between human adipose-derived and mesenchymal-stromal cells despite similar differentiation potentials, Exp Cell Res. 314 (2008) 1575-1584.

24. S. Kern, H. Eichler, J. Stoeve, H. Kluter, K. Bieback, Comparative analysis of mesenchymal stem cells from bone marrow, umbilical cord blood, or adipose tissue, Stem Cells. 24 (2006) 1294-1301.

25. W. Wagner, F. Wein, A. Seckinger, M. Frankhauser, U. Wirkner, U. Krause, J. Blake, C. Schwager, V. Eckstein, W. Ansorge, A.D. Ho, Comparative characteristics of mesenchymal stem cells from human bone marrow, adipose tissue, and umbilical cord blood, Exp Hematol. 33 (2005) 1402-1416.

26. D.G. Phinney, K. Hill, C. Michelson, M. DuTreil, C. Hughes, S. Humphries, R. Wilkinson, M. Baddoo, E. Bayly, Biological activities encoded by the murine mesenchymal stem cell transcriptome provide a basis for their developmental potential and broad therapeutic efficacy, Stem Cells. 24 (2006) 186-198.

27. M.S. Tsai, S.M. Hwang, K.D. Chen, Y.S. Lee, L.W. Hsu, Y.J. Chang, C.N. Wang, H.H. Peng, Y.L. Chang, A.S. Chao, S.D. Chang, K.D. Lee, T.H. Wang, H.S. Wang, Y.K. Soong, Functional network analysis of the transcriptomes of mesenchymal stem cells derived from amniotic fluid, amniotic membrane, cord blood, and bone marrow, Stem Cells. 25 (2007) 2511-2523.

28. L. da Silva Meirelles, A.I. Caplan, N.B. Nardi, In search of the in vivo identity of mesenchymal stem cells, Stem Cells. 26 (2008) 2287-2299.

29. C.M. Huang, C.C. Wang, S. Barnes, C.A. Elmets, In vivo detection of secreted proteins from wounded skin using capillary ultrafiltration probes and mass spectrometric proteomics, Proteomics. 6 (2006) 5805-5814.

30. S.H. Lee, M.J. Son, S.H. Oh, S.B. Rho, K. Park, Y.J. Kim, M.S. Park, J.H. Lee, Thymosin {beta}(10) inhibits angiogenesis and tumor growth by interfering with Ras function, Cancer Res. 65 (2005) 137-148.

31. N. Lapteva, Y. Ando, M. Nieda, H. Hohjoh, M. Okai, A. Kikuchi, G. Dymshits, Y. Ishikawa, T. Juji, K. Tokunaga, Profiling of genes expressed in human monocytes and monocyte-derived dendritic cells using cDNA expression array, Br J Haematol. 114 (2001) 191-197.

32. D. Califano, C. Monaco, G. Santelli, A. Giuliano, M.L. Veronese, M.T. Berlingieri, V. de Franciscis, N. Berger, F. Trapasso, M. Santoro, G. Viglietto, A. Fusco, Thymosin beta-10 gene overexpression correlated with the highly malignant neoplastic phenotype of transformed thyroid cells in vivo and in vitro, Cancer Res. 58 (1998) 823-828.

33. D.T. Covas, R.A. Panepucci, A.M. Fontes, W.A. Silva, Jr., M.D. Orellana, M.C. Freitas, L. Neder, A.R. Santos, L.C. Peres, M.C. Jamur, M.A. Zago, Multipotent mesenchymal stromal cells obtained from diverse human tissues share functional properties and gene-expression profile with CD146+ perivascular cells and fibroblasts, Exp Hematol. 36 (2008) 642-654.

34. F.J. Muller, L.C. Laurent, D. Kostka, I. Ulitsky, R. Williams, C. Lu, I.H. Park, M.S. Rao, R. Shamir, P.H. Schwartz, N.O. Schmidt, J.F. Loring, Regulatory networks define phenotypic classes of human stem cell lines, Nature. 455 (2008) 401-405.

35. J.A. Kode, S. Mukherjee, M.V. Joglekar, A.A. Hardikar, Mesenchymal stem cells: immunobiology and role in immunomodulation and tissue regeneration, Cytotherapy. 11 (2009) 377-391.

36. G. Xu, Y. Zhang, L. Zhang, G. Ren, Y. Shi, Bone marrow stromal cells induce apoptosis of lymphoma cells in the presence of IFNgamma and TNF by producing nitric oxide, Biochem Biophys Res Commun. 375 (2008) 666-670.

37. C. Wiese, A. Rolletschek, G. Kania, P. Blyszczuk, K.V. Tarasov, Y. Tarasova, R.P. Wersto, K.R. Boheler, A.M. Wobus, Nestin expression--a property of multi-lineage progenitor cells?, Cell Mol Life Sci. 61 (2004) 2510-2522.

38. J.A. Oliver, O. Maarouf, F.H. Cheema, T.P. Martens, Q. Al-Awqati, The renal papilla is a niche for adult kidney stem cells, J Clin Invest. 114 (2004) 795-804.

39. D. Patschan, T. Michurina, H.K. Shi, S. Dolff, S.V. Brodsky, T. Vasilieva, L. Cohen-Gould, J. Winaver, P.N. Chander, G. Enikolopov, M.S. Goligorsky, Normal distribution and medullary-to-cortical shift of Nestin-expressing cells in acute renal ischemia, Kidney Int. 71 (2007) 744-754.

40. Q. Lin, J. Schwarz, C. Bucana, E.N. Olson, Control of mouse cardiac morphogenesis and myogenesis by transcription factor MEF2C, Science. 276 (1997) 1404-1407.

41. E. Dodou, M.P. Verzi, J.P. Anderson, S.M. Xu, B.L. Black, Mef2c is a direct transcriptional target of ISL1 and GATA factors in the anterior heart field during mouse embryonic development, Development. 131 (2004) 3931-3942.

42. C.T. Basson, D.R. Bachinsky, R.C. Lin, T. Levi, J.A. Elkins, J. Soults, D. Grayzel, E. Kroumpouzou, T.A. Traill, J. Leblanc-Straceski, B. Renault, R. Kucherlapati, J.G. Seidman, C.E. Seidman, Mutations in human TBX5 [corrected] cause limb and cardiac malformation in Holt-Oram syndrome, Nat Genet. 15 (1997) 30-35.

43. L.A. Naiche, V.E. Papaioannou, Tbx4 is not required for hindlimb identity or post-bud hindlimb outgrowth, Development. 134 (2007) 93-103.

44. B.S. Mankoo, S. Skuntz, I. Harrigan, E. Grigorieva, A. Candia, C.V. Wright, H. Arnheiter, V. Pachnis, The concerted action of Meox homeobox genes is required upstream of genetic pathways essential for the formation, patterning and differentiation of somites, Development. 130 (2003) 4655-4664.

45. S. Skuntz, B. Mankoo, M.T. Nguyen, E. Hustert, A. Nakayama, E. Tournier-Lasserve, C.V. Wright, V. Pachnis, K. Bharti, H. Arnheiter, Lack of the mesodermal homeodomain protein MEOX1 disrupts sclerotome polarity and leads to a remodeling of the cranio-cervical joints of the axial skeleton, Dev Biol. 332 (2009) 383-395.

46. A.I. Caplan, Mesenchymal stem cells, J Orthop Res. 9 (1991) 641-650.

47. D. Menicanin, P.M. Bartold, A.C. Zannettino, S. Gronthos, Genomic profiling of mesenchymal stem cells, Stem Cell Rev. 5 (2009) 36-50.

48. K. Kollar, M.M. Cook, K. Atkinson, G. Brooke, Molecular mechanisms involved in mesenchymal stem cell migration to the site of acute myocardial infarction, Int J Cell Biol. 2009 (2009) 904682.

49. T. Tondreau, N. Meuleman, B. Stamatopoulos, C. De Bruyn, A. Delforge, M. Dejeneffe, P. Martiat, D. Bron, L. Lagneaux, In vitro study of matrix metalloproteinase/tissue inhibitor of metalloproteinase production by mesenchymal stromal cells in response to inflammatory cytokines: the role of their migration in injured tissues, Cytotherapy. 11 (2009) 559-569.

50. C. Ries, V. Egea, M. Karow, H. Kolb, M. Jochum, P. Neth, MMP-2, MT1-MMP, and TIMP-2 are essential for the invasive capacity of human mesenchymal stem cells: differential regulation by inflammatory cytokines, Blood. 109 (2007) 4055-4063.

51. X.X. Jiang, Y.F. Su, X.S. Li, Y. Zhang, Y. Wu, N. Mao, Human fetal heart-derived adherent cells with characteristics similar to mesenchymal progenitor cells, Zhongguo Shi Yan Xue Ye Xue Za Zhi. 14 (2006) 1191-1194.

52. M.J. Hoogduijn, M.J. Crop, A.M. Peeters, G.J. Van Osch, A.H. Balk, J.N. Ijzermans, W. Weimar, C.C. Baan, Human heart, spleen, and perirenal fat-derived mesenchymal stem cells have immunomodulatory capacities, Stem Cells Dev. 16 (2007) 597-604.

53. T. Miyazaki, U. Muller, K.S. Campbell, Normal development but differentially altered proliferative responses of lymphocytes in mice lacking CD81, EMBO J. 16 (1997) 4217-4225.

54. R.C. Lai, F. Arslan, M.M. Lee, N.S. Sze, A. Choo, T.S. Chen, M. Salto-Tellez, L. Timmers, C.N. Lee, R.M. El Oakley, G. Pasterkamp, D.P. de Kleijn, S.K. Lim, Exosome

secreted by MSC reduces myocardial ischemia/reperfusion injury, Stem Cell Res. 4 (2010) 214-222.

55. U. Riekstina, I. Cakstina, V. Parfejevs, M. Hoogduijn, G. Jankovskis, I. Muiznieks, R. Muceniece, J. Ancans, Embryonic stem cell marker expression pattern in human mesenchymal stem cells derived from bone marrow, adipose tissue, heart and dermis, Stem Cell Rev. 5 (2009) 378-386.

56. S.J. Greco, K. Liu, P. Rameshwar, Functional similarities among genes regulated by OCT4 in human mesenchymal and embryonic stem cells, Stem Cells. 25 (2007) 3143-3154.

57. P. Barraud, S. Stott, K. Mollgard, M. Parmar, A. Bjorklund, In vitro characterization of a human neural progenitor cell coexpressing SSEA4 and CD133, J Neurosci Res. 85 (2007) 250-259.

58. C.J. Lengner, F.D. Camargo, K. Hochedlinger, G.G. Welstead, S. Zaidi, S. Gokhale, H.R. Scholer, A. Tomilin, R. Jaenisch, Oct4 expression is not required for mouse somatic stem cell self-renewal, Cell Stem Cell. 1 (2007) 403-415.

59. X. Yan, H. Qin, C. Qu, R.S. Tuan, S. Shi, G.T. Huang, iPS cells reprogrammed from human mesenchymal-like stem/progenitor cells of dental tissue origin, Stem Cells Dev. 19 (2009) 469-480.

60. J. Cai, W. Li, H. Su, D. Qin, J. Yang, F. Zhu, J. Xu, W. He, X. Guo, K. Labuda, A. Peterbauer, S. Wolbank, M. Zhong, Z. Li, W. Wu, K.F. So, H. Redl, L. Zeng, M.A. Esteban, D. Pei, Generation of human induced pluripotent stem cells from umbilical cord matrix and amniotic membrane mesenchymal cells, J Biol Chem. 285 (2010) 11227-11234.

61. R.G. Tilton, Capillary pericytes: perspectives and future trends, J Electron Microsc Tech. 19 (1991) 327-344.

62. J. Yamashita, H. Itoh, M. Hirashima, M. Ogawa, S. Nishikawa, T. Yurugi, M. Naito, K. Nakao, Flk1-positive cells derived from embryonic stem cells serve as vascular progenitors, Nature. 408 (2000) 92-96.

63. D. Bexell, S. Gunnarsson, A. Tormin, A. Darabi, D. Gisselsson, L. Roybon, S. Scheding, J. Bengzon, Bone marrow multipotent mesenchymal stroma cells act as pericyte-like migratory vehicles in experimental gliomas, Mol Ther. 17 (2009) 183-190.

64. C. Sundberg, M. Kowanetz, L.F. Brown, M. Detmar, H.F. Dvorak, Stable expression of angiopoietin-1 and other markers by cultured pericytes: phenotypic similarities to a subpopulation of cells in maturing vessels during later stages of angiogenesis in vivo, Lab Invest. 82 (2002) 387-401.

65. B. Brachvogel, H. Moch, F. Pausch, U. Schlotzer-Schrehardt, C. Hofmann, R. Hallmann, K. von der Mark, T. Winkler, E. Poschl, Perivascular cells expressing annexin A5 define a novel mesenchymal stem cell-like population with the capacity to differentiate into multiple mesenchymal lineages, Development. 132 (2005) 2657-2668.

66. D.J. Pennisi, L. Wilkinson, G. Kolle, M.L. Sohaskey, K. Gillinder, M.J. Piper, J.W. McAvoy, F.J. Lovicu, M.H. Little, Crim1KST264/KST264 mice display a disruption of the Crim1 gene resulting in perinatal lethality with defects in multiple organ systems, Dev Dyn. 236 (2007) 502-511.

67. G.K. Smyth, Limma: linear models for microarray data, eds. Bioinformatics and Computational Biology Solutions using R and Bioconductor, New York: Springer, 2005: 397-420.

68. P. Du, W.A. Kibbe, S.M. Lin, lumi: a pipeline for processing Illumina microarray, Bioinformatics. 24 (2008) 1547-1548.

69. G.K. Smyth, Linear models and empirical bayes methods for assessing differential expression in microarray experiments, Stat Appl Genet Mol Biol. 3 (2004) Article3.

70. M.E. Christensen, B.E. Turner, L.J. Sinfield, H. Cullup, K. Kollar, N.J. Waterhouse, D.N. Hart, K. Atkinson, A.M. Rice**.** Infusion of allogeneic mesenchymal stromal cells can delay but not prevent GVHD after murine transplantation. Haematologica 95(2010) 2102-10.

Figure Legends

Figure 1. Experimental plan and analysis of subsequent morphology and multipotency of tissue-specific MSC-like populations from heart and kidney. A. Experimental flow chart indicating the initial isolation of subfractions able to generate CFU-F followed by uniform passaging prior to comparative characterisation. **B.** Analysis of the differentiative capacity of the three populations after passage. **a-c)** Light microscopy of adherent cultures. **d-f)** Light microscopy of Giemsa-stained cytospin preparations. **g-i)** Oil red-O staining of lipid droplets after 21 day culture in adipogenic media. **j-l)** Alizarin red staining of osteoid matrix after 21 day culture in osteogenic media. **m-o)** Alcian blue staining of proteoglycans after 21 day pellet culture in chondrogenic media. Scale bars: A-C, 50μM; D-F, 100μM, G-H, 50μM, J-L, 200μm; M-O, 500μM.

Figure 2. Comprehensive CD epitope profiling of bmMSC, cCFU-F and kCFU-F populations. A) Clustered heat map representation of data from (total number) cell surface antigens expressed as percentage cells positive for each epitope. Increasing color intensity indicates an increasing percentage of cells positive. Epitopes in common or enriched in kCFU-F or cCFU-F are shown in expanded lists alongside heat map. **B)** Graphical representative of CD profiling for all epitopes where >20% of any cell populations was positive. Values are an average of 2 replicates with the same cell line.

Figure 3. Correlation of gene expression profile between bmMSC, cCFU-F and kCFU-F populations. A) Pair-wise correlation of gene expression profiles (medium-high expression genes only). **B)** Gene expression heat map of 327 mouse orthologs to defined Plurinet genes in bmMSC, cCFU-F and kCFU-F. Colour key shown in upper left corner (Log2). **C)** Representation of the spatial location of Plurinet gene-encoded proteins expressed in all three

MSC-like populations. Only the genes that had expression above background fluorescence are shown in the network. Level of expression for listed genes is as for panel B. Grey indicates a gene within the network whose expression was not detected in any population at a level above background.

Figure 4. Differential function and gene expression profile of bmMSC, cCFU-F and kCFU-F. A) Mixed lymphocyte reaction assay of *in vitro* immune suppression of T-cell alloreactivity. The ability of each of the three MSC-like populations to suppress proliferation of T-cells activated in response to BALB/c [H-2^d] stimulator cells. R+S = baseline proliferation (^{3}H-thymidine uptake) of activated T-cells in the presence of stimulator cells. $3x10^3$ or $3x10^4$ cells of each MSC-like population were co-cultured with responders and stimulators. Error bars represent standard error of the mean, n = 3 to 5. Statistics calculated using one way analysis of variance with post hoc Dunnett's test (comparing all samples to controls). *** = P>0.001, NS= not significantly different. **B)** Heat map representing the relative expression of 6533 genes differentially expressed between the three MSC-like populations. Blue – reduced relative expression, red – elevated relative expression. **C)** Venn diagram of differentially expressed genes from B). Venn diagram showing numbers of genes statistically differentially expressed by fold change. **D)** Representation of the most differentially up-regulated genes present in each of the three MSC-like populations. **E)** Representation of the most differentially down-regulated genes present in each of the three MSC-like populations.

Figure 5. Differential epitope density between bmMSC, cCFU-F and kCFU-F populations and correlations between gene expression and immunophenotype. A) Graph of fold change in fluorescence intensity (representing relative epitope density) for all epitopes where at least one population displayed a fold change of >20. **B)** Graph of fold change in

fluorescence intensity for all epitopes detected on >50% of all three populations. **C)** Graph indicating the level of gene expression (mean fluorescence intensity) for all genes encoding CD epitopes detected as present on >40% of cells in any given population. Epitope names are listed rather than the gene symbol of the encoding gene. Expression of CD201 and CD61 showed an Illumina detection score >0 (not expressed above background). Gene expression for CD24 was not used as it mapped to more than one location in the genome. Gene expression could not distinguish between CD90 and CD90.2 hence the intensity displayed is for an oligonuclotide mapping to Thy1, which encodes both protein isoforms. (There are two CD71 label on the graph? Fig 5C)

Table legends.

Table 1. Gene family / pathways in common between the three MSC-like populations based upon microarray expression profiling.

Table 2. Five most population-specific gene transcripts for each of the three populations examined. Genes showing the greatest enrichment of expression in comparison with both other populations (enriched genes) were defined as populations specific if their relative expression was >5 fold higher than the remaining populations, both of which showed expression of <200RFU (relative fluorescence units) for the same gene.

Figure 1

Click here to download high resolution image

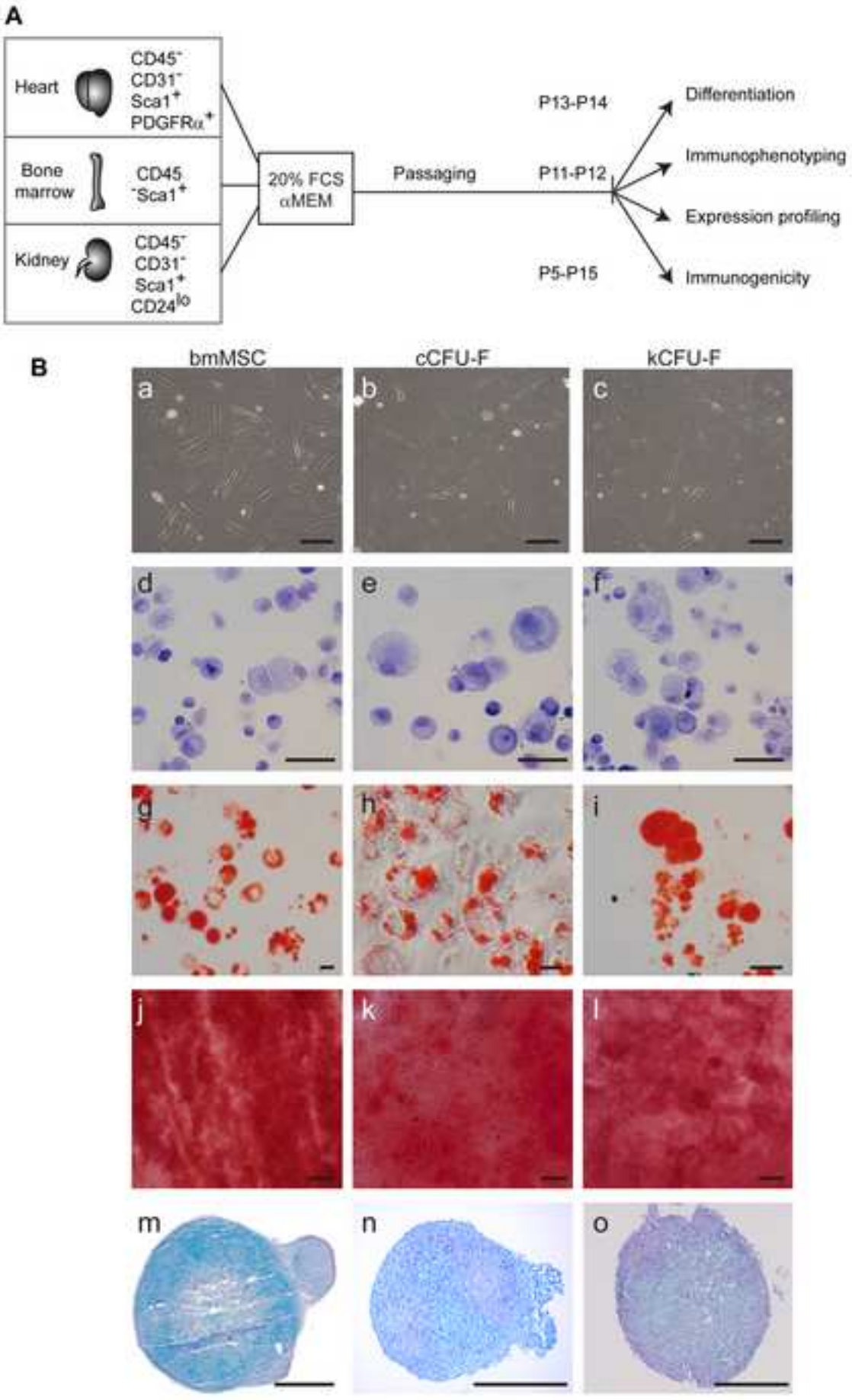

Figure 2

Click here to download high resolution image

Figure 2

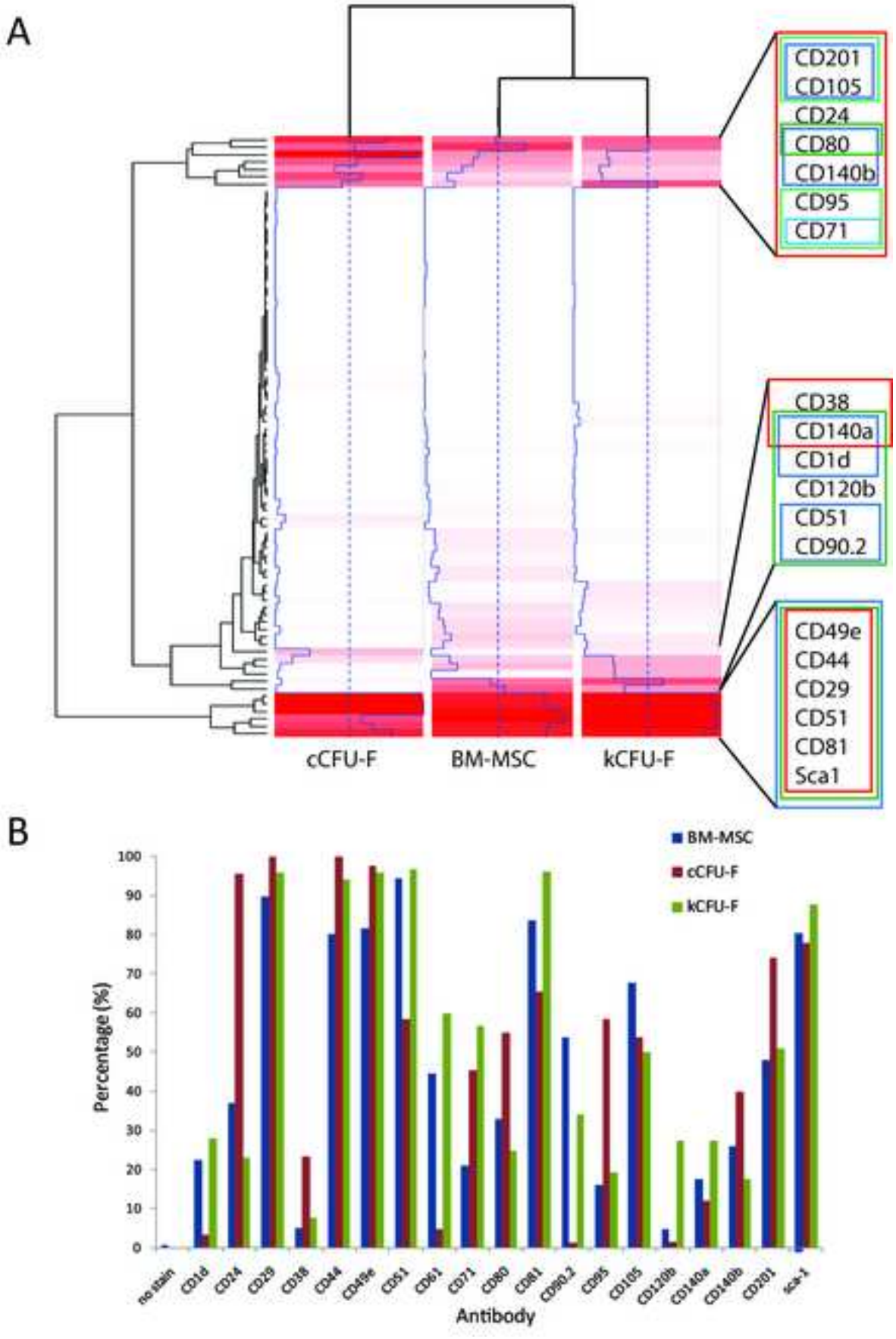

Figure 3

Click here to download high resolution image

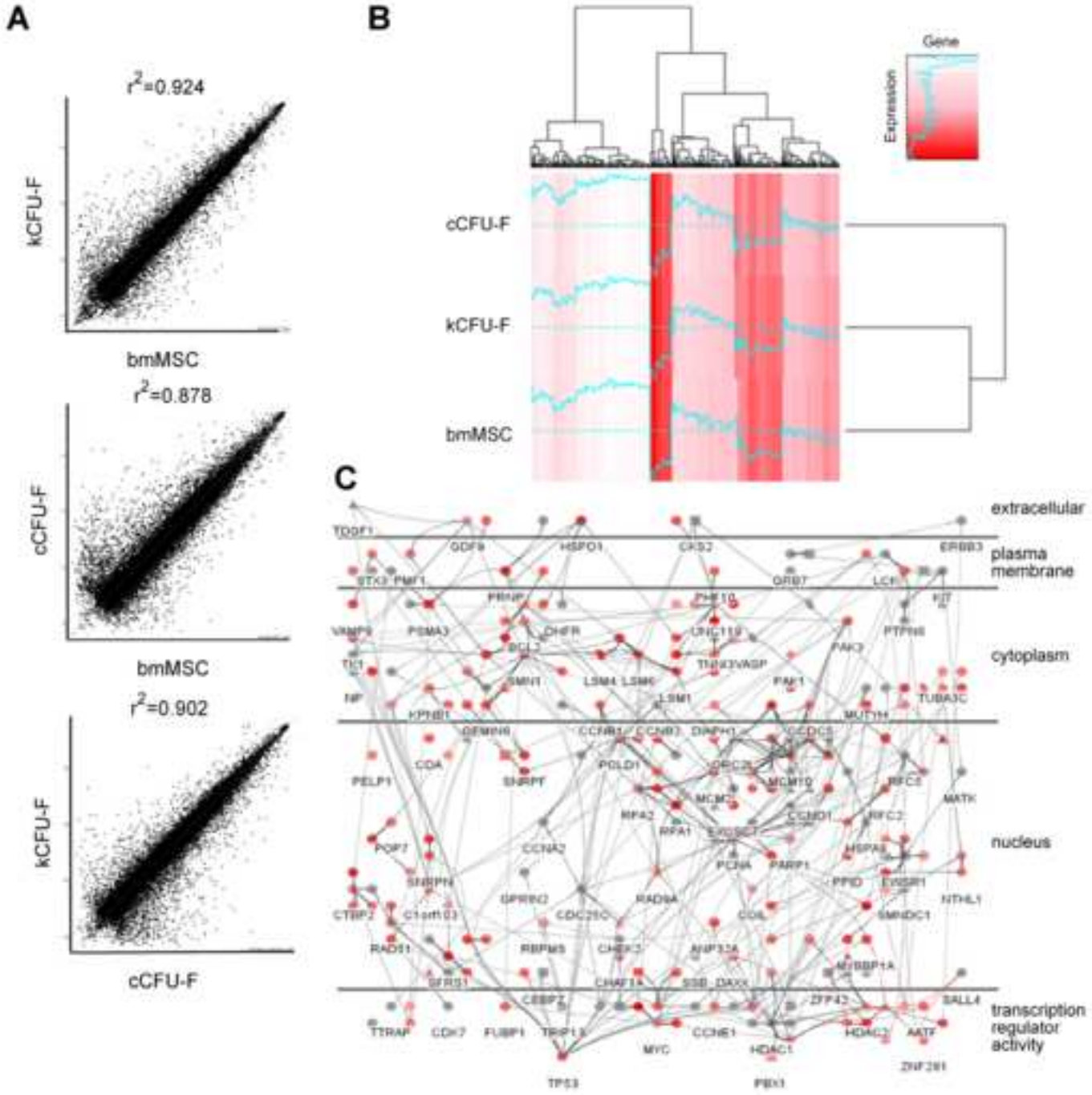

Figure 4

Click here to download high resolution image

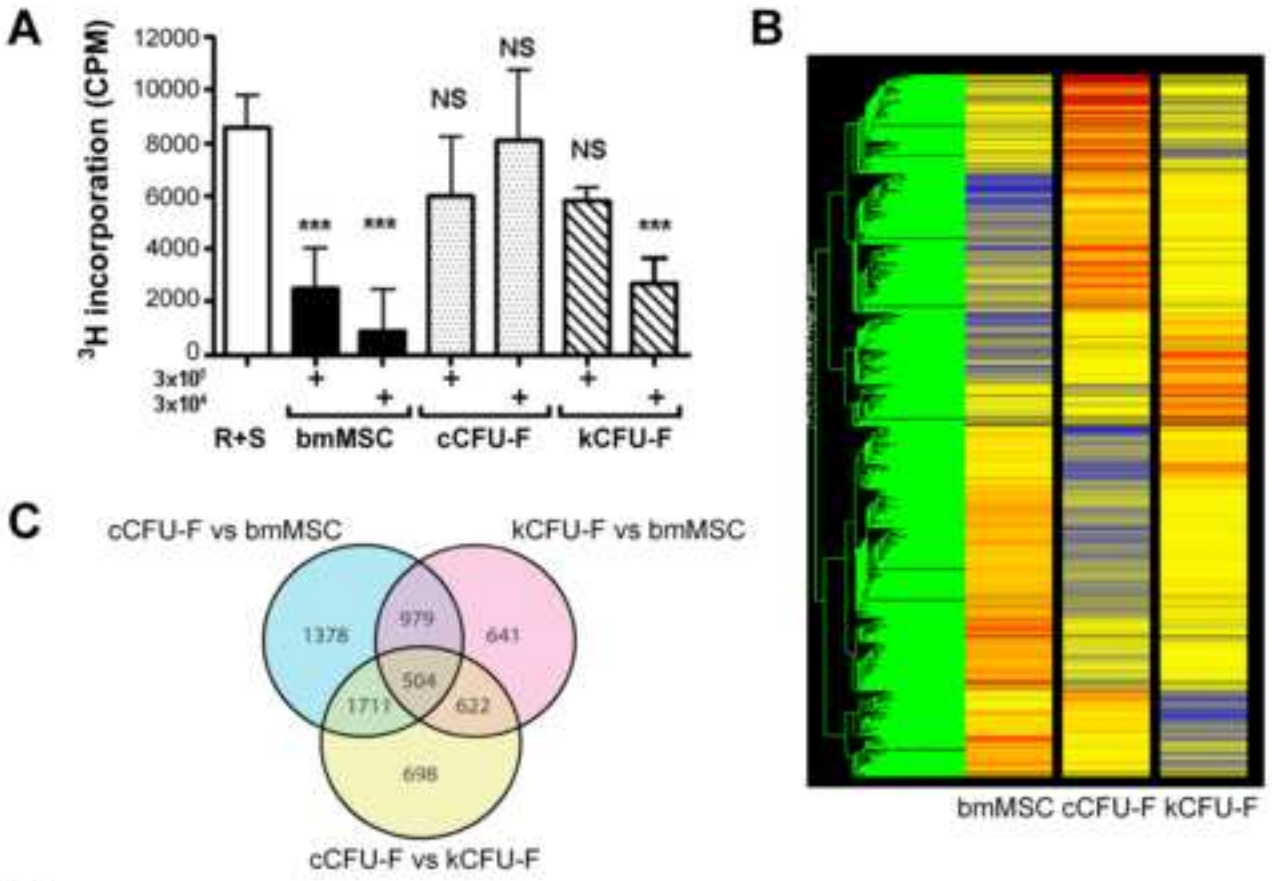

Figure 5

Click here to download high resolution image

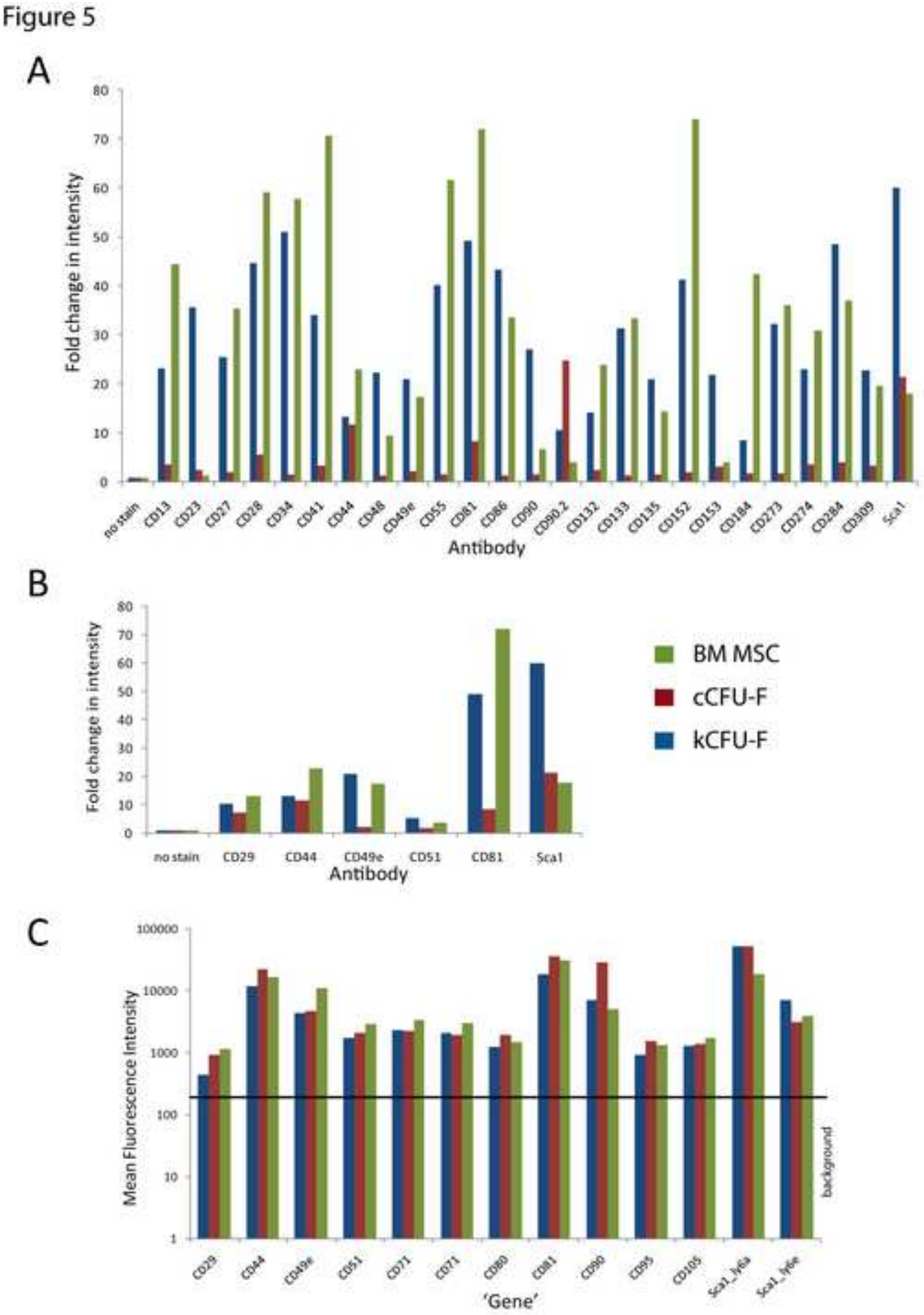

Table 1.

Pathway	Predicted expressed proteins
Immunity associated proteins	CD1d1, CD binding protein, CD3 epsilon associated protein, CD8b, CD24, CD80, CD81, CD99, IL-1 receptor type 1 (CD121a), IL-3 receptor a (CD123), CD124, CXCL12 receptor (CD184), CD201, CD276, IL-1, ILf2, IL6st
Cell adhesion	CD44, CD29, integrin alpha 5 chain, CD106, CD51(vitronectin receptor), integrin α11, integrin alpha FG-GAP repeat containing 2**,** integrin αFG-GAP repeat containing 3, integrin β1 binding protein 1, integrin β 5, and integrin β-like 1
BMP pathway	Bmp1, Bmper, Bmpr1A, Bmpr1B
CXC chemokines	Ccxc1, Cxcl12 (SDF-1), Cx3cl1 (fractalkine), Ccl2, Ccl7 and Ccl25
Homeobox transcription factors	HoxA2, HoxA4, HoxA5, HoxA7, HoxB2, HoxB4, HoxB5, HoxB6, HoxB7
CD epitope encoding genes	Tetraspanin (CD9), CD14, CD24, thrombospondin receptor (CD47), CD49e, CD51, CD59a, CD63, transferrin receptor (CD71), CD80, CD81, CD82, Fas receptor (CD95), CD97, CD109, TNF receptor (CD120), CD124, PGFRα (CD140a), PGFRβ (CD140b), Mcam (CD146) CD151, CD164, CD184, CD201, CD221 IGF-1 receptor (CD221), endosialin (CD248; CD146L).
Metalloproteinases	Mmp2, Mmp14, Mmp23, Mmp24
TIMPS	Timp1, Timp2, Timp3

Table 2.

Bone marrow MSC specific genes			
Gene name (symbol)	**bmMSC Raw RFU**	**cCFU-F Raw RFU**	**kCFU-F Raw RFU**
Ubiquitin specific peptidase 18 (USP18)	937.12	34.63	39.11
DEXH (Asp-Glu-X-His) box polypeptide 58 (DHX58)	742.94	42.40	30.41
2'-5' oligoadenylate synthetase-like 2 (OASL2)	2471.00	95.86	163.54
Radical S-adenosyl methionine domain containing 2 (RSAD2)	852.07	64.12	33.6
Kininogen 2 (Kng2)	1393.55	161.86	155.10
Cardiac cCFU-F specific genes			
Gene name (symbol)	**cCFU-F Raw RFU**	**kCFU-F Raw RFU**	**bmMSC Raw RFU**
Serine (or cysteine) peptidase inhibitor, clade A, member 3N (Serpina3n)	11937.01	12.13	23.66
G-protein coupled receptor 88 (Gpr88)	2710.62	13.29	9.26
Fibroblast growth factor 10 (Fgf10)	1204.88	8.85	11.01
LOC100046120 (similar to clusterin)	1602.12	11.60	15.18
SLIT and NTRK-like family, member 5 (Slitrk5)	1819.02	19.77	14.71
Kidney kCFU-F specific genes			
Gene name (symbol)	**kCFU-F Raw RFU**	**bmMSC Raw RFU**	**cCFU-F Raw RFU**
Natriuretic peptide precursor type B (NPPB)	1132.44	38.67	105.62
LOC100044395 (similar to RNA binding protein gene with multiple splicing)	831.74	99.50	63.39
Sciellin (SCEL)	559.75	8.54	66.58
Williams-Beuren syndrome chromosome region 17 homolog (human) (WBSCR17)	616.02	73.79	71.70
LOC233466	942.52	179.03	93.15

Supplementary Table 1

Click here to download Supplementary Material: Supplementary Table 1 revised.docx

Supplementary Table 2

Click here to download Supplementary Material: Supplementary Table 2 (2Aug2011).doc

Supplementary Table 3

Click here to download Supplementary Material: Supplementary Table 3 final.doc

Supplementary Table 4

Click here to download Supplementary Material: Supplementary Table 4 revised.doc

Supplementary Table 5

Click here to download Supplementary Material: Supplementary Table 5 final.docx

Supplementary Table 6

Click here to download Supplementary Material: Supplementary Table 6 final.docx

Supplementary Table 7

Click here to download Supplementary Material: Supplementary Table 7 final.docx

Supplementary Table 8

Click here to download Supplementary Material: Supplementary Table 8 final.docx

Supplementary Figure 1

Click here to download Supplementary Material: Supplementary Figure S1 revised.tif

Supplementary Figure 2

Click here to download Supplementary Material: Supplementary Figure S2 revised.tif

Supplementary Figure 3

Click here to download Supplementary Material: Supplementary Figure S3 revised.tif

Supplementary Figure 4

Click here to download Supplementary Material: Supplementary Figure S4 revised.tif

Supplementary Figure 5

Click here to download Supplementary Material: Supplementary Fig S5.tif

Supplementary Data

Click here to download Supplementary Material: Supplementary Data revised 30 July.docx

***Highlights**

- Direct comparison of the phenotype of MSCs isolated from heart and kidney compared with those isolated from bone marrow
- All populations showed positive staining for known MSC markers (Sca1, CD90.2, CD29, CD44, CD24, CD49e, CD51, CD81, CD105)
- Strong congruence between immunophenotype and gene expression between all populations, although immunosuppressive function varied
- Despite similarity, differences do exist at the level of epitope density and gene expression which may reflect a tissue of origin memory

A Self Built PDF of Figures ONLY (no figure legends)

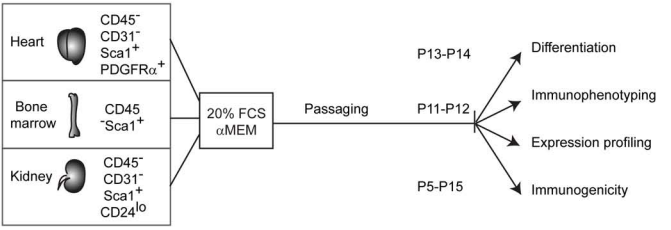

B

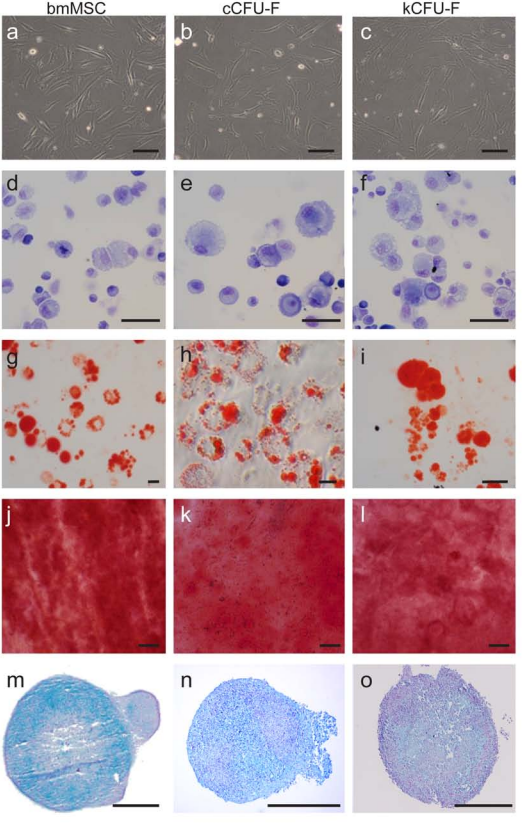

Figure 2

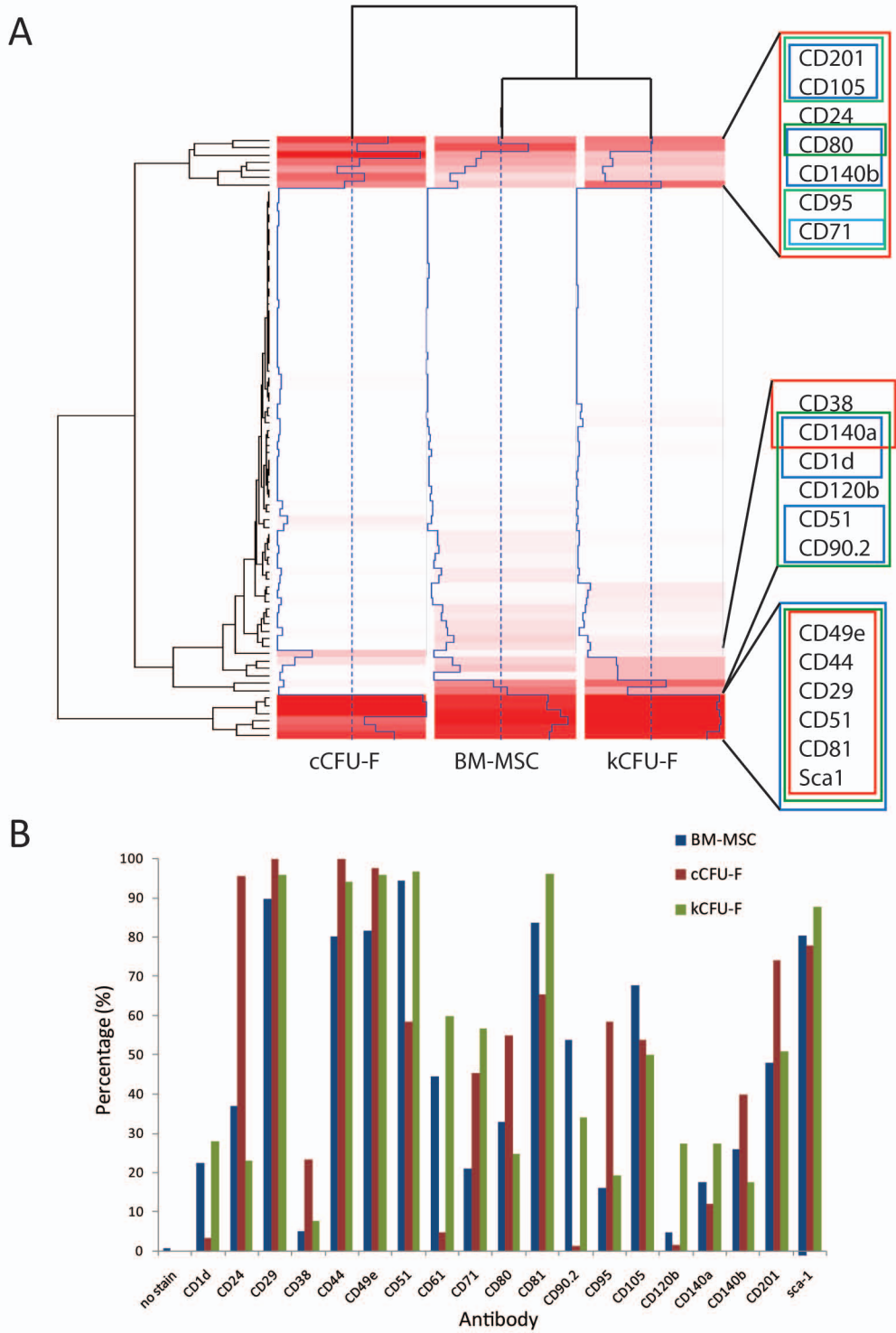
A
CD201
CD105
CD24
CD80
CD140b
CD95
CD71
CD38
CD140a
CD1d
CD120b
CD51
CD90.2
CD49e
CD44
CD29
CD51
CD81
Sca1
cCFU-F
BM-MSC
kCFU-F
B
BM-MSC
cCFU-F
kCFU-F
Percentage (%)
100
90
80
70
60
50
40
30
20
10
0
no stain
CD1d
CD24
CD29
CD38
CD44
CD49e
CD51
CD61
CD71
CD80
CD81
CD90.2
CD95
CD105
CD120b
CD140a
CD140b
CD201
sca-1
Antibody

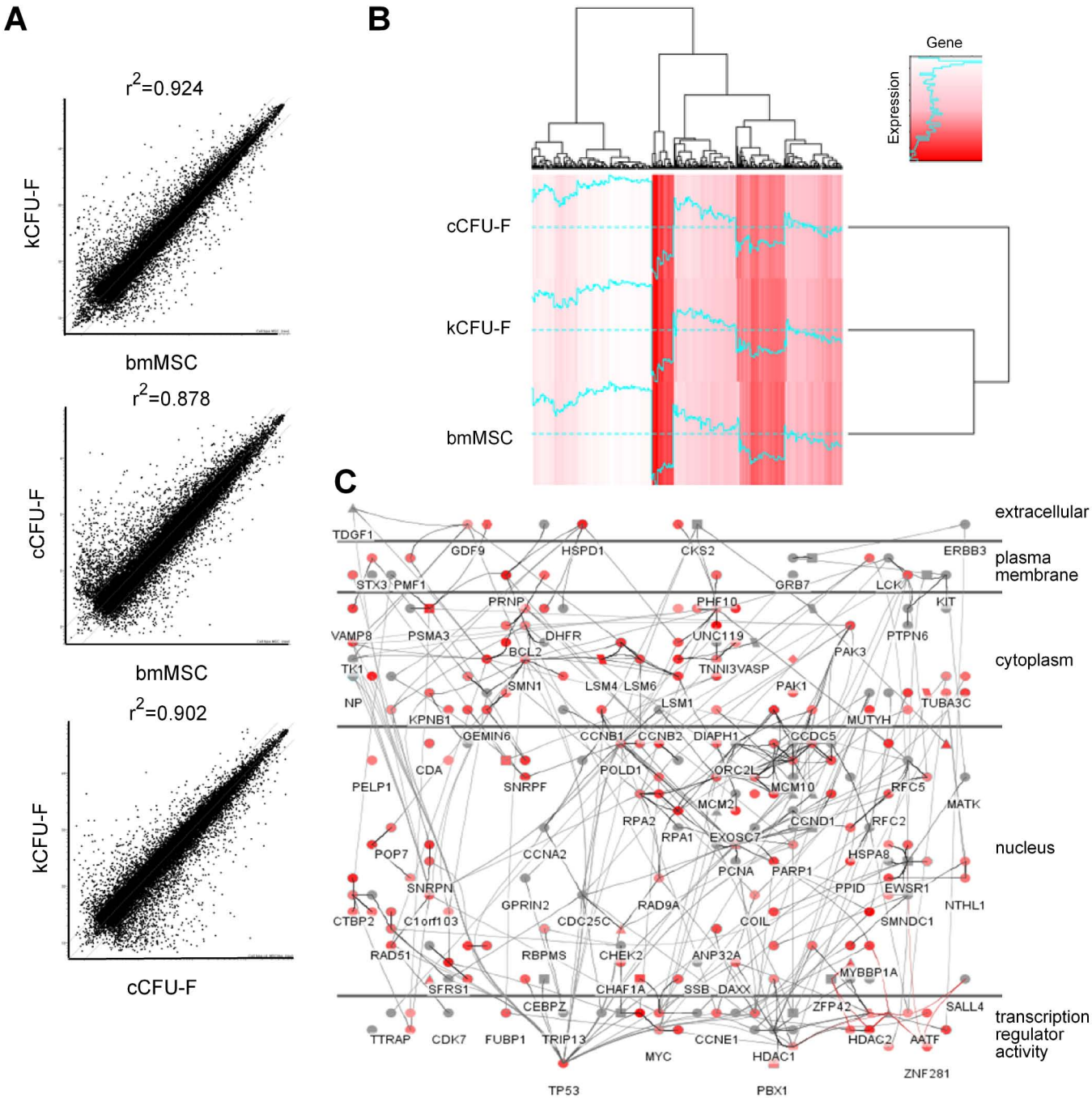
A
r2=0.924
kCFU-F
bmMSC
r2=0.878
cCFU-F
bmMSC
r2=0.902
kCFU-F
cCFU-F
B
Gene
Expression
cCFU-F
kCFU-F
bmMSC
C
extracellular
plasma membrane
cytoplasm
nucleus
transcription regulator activity
TDGF1
GDF9
HSPD1
CKS2
ERBB3
STX3
PMF1
GRB7
LCK
KIT
PRNP
PHF10
VAMP8
PSMA3
DHFR
UNC119
PTPN6
BCL2
PAK3
TK1
TNNI3VASP
SMN1
LSM4
LSM6
PAK1
NP
KPNB1
LSM1
TUBA3C
MUTYH
GEMIN6
CCNB1
CCNB2
DIAPH1
CCDC5
CDA
POLD1
ORC2L
PELP1
SNRPF
MCM10
RFC5
MCM2
MATK
RPA2
CCND1
RFC2
RPA1
EXOSC7
POP7
CCNA2
HSPA8
PCNA
PARP1
SNRPN
PPID
EWSR1
GPRIN2
RAD9A
NTHL1
CTBP2
C1orf103
CDC25C
COIL
SMNDC1
RAD51
RBPMS
CHEK2
ANP32A
MYBBP1A
SFRS1
CHAF1A
SSB
DAXX
CEBPZ
ZFP42
SALL4
TTRAP
CDK7
FUBP1
TRIP13
CCNE1
HDAC2
AATF
MYC
HDAC1
ZNF281
TP53
PBX1

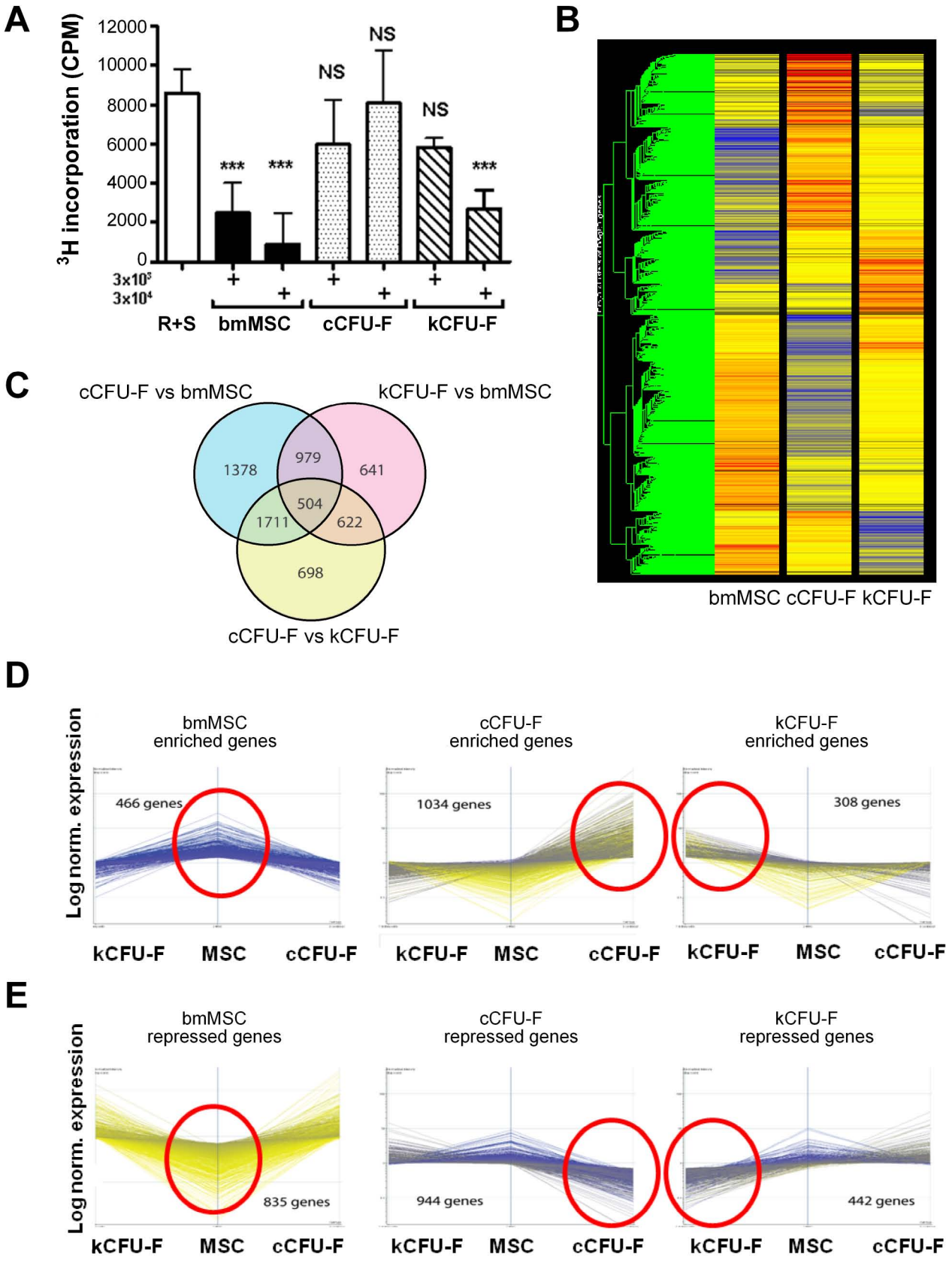
A
^{3}H incorporation (CPM)
12000
10000
8000
6000
4000
2000
0
NS
NS
NS
***
***
***
3x10^3
3x10^4
+
+
+
+
+
+
R+S
bmMSC
cCFU-F
kCFU-F
B
bmMSC cCFU-F kCFU-F
C
cCFU-F vs bmMSC
kCFU-F vs bmMSC
1378
979
641
504
1711
622
698
cCFU-F vs kCFU-F
D
Log norm. expression
bmMSC
enriched genes
466 genes
kCFU-F
MSC
cCFU-F
cCFU-F
enriched genes
1034 genes
kCFU-F
MSC
cCFU-F
kCFU-F
enriched genes
308 genes
kCFU-F
MSC
cCFU-F
E
Log norm. expression
bmMSC
repressed genes
835 genes
kCFU-F
MSC
cCFU-F
cCFU-F
repressed genes
944 genes
kCFU-F
MSC
cCFU-F
kCFU-F
repressed genes
442 genes
kCFU-F
MSC
cCFU-F

Figure 5

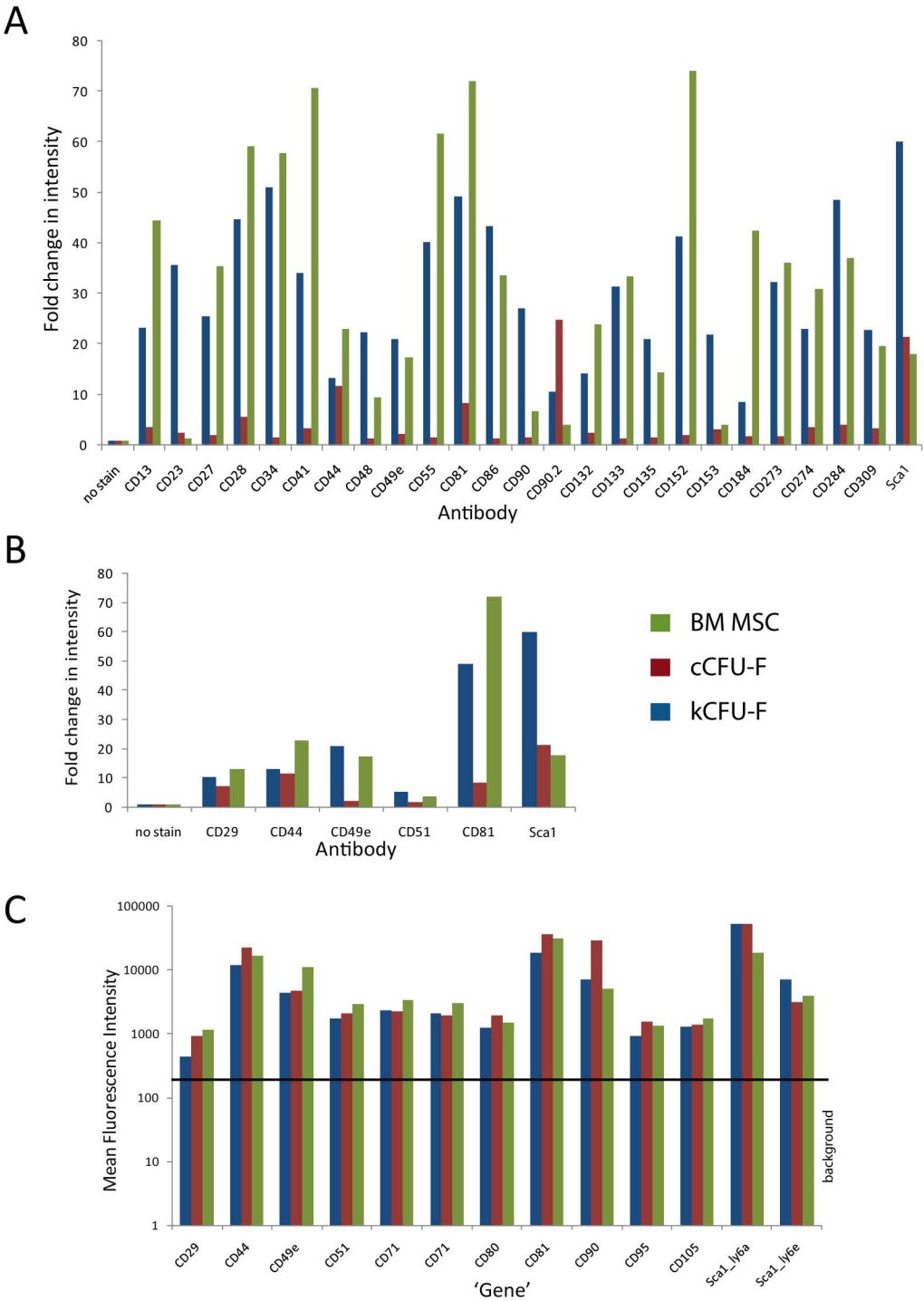
A
Fold change in intensity
80
70
60
50
40
30
20
10
0
no stain
CD13
CD23
CD27
CD28
CD34
CD41
CD44
CD48
CD49e
CD55
CD81
CD86
CD90
CD90.2
CD132
CD133
CD135
CD152
CD153
CD184
CD273
CD274
CD284
CD309
Sca1
Antibody
B
Fold change in intensity
80
70
60
50
40
30
20
10
0
no stain
CD29
CD44
CD49e
CD51
CD81
Sca1
Antibody
BM MSC
cCFU-F
kCFU-F
C
Mean Fluorescence Intensity
100000
10000
1000
100
10
1
background
CD29
CD44
CD49e
CD51
CD71
CD71
CD80
CD81
CD90
CD95
CD105
Sca1_ly6a
Sca1_ly6e
'Gene'